European Journal of Taxonomy 981: 155–188
https://doi.org/10.5852/ejt.2025.981.2823
ISSN 2118-9773
www.europeanjournaloftaxonomy.eu
2025 · Vecchi M. *et al.*

Research article

urn:lsid:zoobank.org:pub:6BACE4E9-942A-4A2E-B85C-ADB62E8BB9AB

Taxonomic reanalysis of the genus *Richtersius* (Tardigrada; Eutardigrada), with description of two new species from Italy and Sweden

Matteo VECCHI [1,*], Jakub GODZIEK [2], Reinhardt M. KRISTENSEN [3], Lucia PIEMONTESE [4], Sara CALHIM [5] & Daniel STEC [6]

[1,2,6] Institute of Systematics and Evolution of Animals, Polish Academy of Sciences, Sławkowska 17, 31-016, Kraków, Poland.
[3] Natural History Museum of Denmark, University of Copenhagen, Copenhagen, Denmark.
[4] Independent researcher, Bologna, Italy.
[5] Department of Biological and Environmental Science, University of Jyväskylä, Jyväskylä, Finland.

[*] Corresponding author: matteo.vecchi15@gmail.com
[2] Email: jackobpc@gmail.com
[3] Email: rmkristensen@snm.ku.dk
[4] Email: lucia.piemontese1@gmail.com
[5] Email: s.calhim@gmail.com
[6] Email: daniel_stec@interia.eu

[1] urn:lsid:zoobank.org:author:817A0470-5C95-49C5-8AA8-B731BE0A7CD9
[2] urn:lsid:zoobank.org:author:D8D18430-7C38-4F67-94CB-23E6DA3E3A19
[3] urn:lsid:zoobank.org:author:4BA89040-D79E-41C1-A17C-539FBB9B6BA4
[4] urn:lsid:zoobank.org:author:2830229F-2B64-421C-80D4-0C165C8BEC3F
[5] urn:lsid:zoobank.org:author:B309F420-F7F9-4708-B59E-66880642F93E
[6] urn:lsid:zoobank.org:author:13C435F8-25AB-47DE-B5BB-8CE788E92CF6

Abstract. The tardigrade genus *Richtersius* Pilato & Binda, 1989 has been considered monotypic for more than 30 years since its establishment and is frequently used in experimental studies on physiological adaptations to stress. Only recently, integrative taxonomy has allowed us to disentangle and describe different but similar species. In this study, we provide a taxonomic reanalysis of the genus *Richtersius* with an integrative description of two new species based on light and scanning electron microscopy as well as DNA sequencing of four markers (18S rDNA, 28S rDNA, ITS-2, and COI). *Richtersius nicolai* sp. nov. and *Richtersius ingemari* sp. nov. are distinguished from congeneric species based on a combination of pore density in newborn's dorsal cuticle, egg diameters, placoid sizes and reproductive modes. This reanalysis of the genus *Richtersius* will facilitate the future descriptions of new species and provides a solid taxonomic background for the identification of the species used in experimental research.

Keywords. New species, water bears, morphology, integrative taxonomy.

Vecchi M., Godziek J., Kristensen R.M., Piemontese L., Calhim S. & Stec D. 2025. Taxonomic reanalysis of the genus *Richtersius* (Tardigrada; Eutardigrada), with description of two new species from Italy and Sweden. *European Journal of Taxonomy* 981: 155–188. https://doi.org/10.5852/ejt.2025.981.2823

Introduction

Richtersius Pilato & Binda, 1989 is a tardigrade genus placed within the family Richtersiusidae Guidetti, Schill, Giovannini, Massa, Goldoni, Ebel, Förschler, Rebecchi & Cesari, 2021 (Guidetti *et al.* 2021) and has been considered monotypic for more than 30 years since its establishment (Pilato & Binda 1987, 1989), with one validly recognized and geographically widespread species: *Richtersius coronifer* (Richters, 1903). However, the presence of cryptic diversity was foreshadowed by investigations of physiology, reproductive modes and allozymes in different populations (Jönsson *et al.* 2001; Rebecchi *et al.* 2003). In recent years, various researchers have shown that within *Richtersius*, multiple and phenotypically similar species are present (Guidetti *et al.* 2016; Kayastha *et al.* 2020; Stec *et al.* 2020b; Kiosya & Stec 2022; Pogwizd & Stec 2022). The primary cause for this recent increase in the identification of new species in this genus was the vague and imprecise original description of *R. coronifer* (common in older tardigrade species descriptions) that created a false sense of its ubiquity. This taxonomic issue was addressed by an integrative re-description of the species using modern standards, followed by the establishment of the new neotype (Stec & Michalczyk 2020). The modernized description as well as neotypification of *R. coronifer* allowed the description of three other species in the genus by means of integrative taxonomy (*R. ziemowiti* Kayastha, Berdi, Mioduchowska, Gawlak, Łukasiewicz, Gołdyn, Jędrzejewski & Kaczmarek, 2020 and *R. tertius* Pogwizd & Stec, 2022) or morphology alone (*R. mazepi* Kiosya & Stec, 2022). In this study, we provide a description based on morphology, morphometrics, and DNA data of two new species of *Richtersius* from the Gargano peninsula (Italy) and Öland Island (Sweden) and provide an updated phylogeny for the genus. We also propose Unconfirmed Candidate Species (UCS; Padial *et al.* 2010) names for three undescribed species identified by molecular methods. Finally, in this work we also provide a dichotomous morphological key to all currently recognized species of *Richtersius* to improve their identification in the future.

Material and methods

Samples and specimens

Samples and specimens used in this study are listed in Table 1. Samples were manually collected, desiccated at room temperature and stored in paper bags until processing. Tardigrades and eggs were extracted using standard methods as described in Massa *et al.* (2024).

Microscopy and imaging

Specimens for light microscopy were mounted on microscope slides in a small drop of Hoyer's medium, secured with a cover slip and dried at 50°C for a week. Slides were examined under a Leica DMLB light microscope with phase contrast (PCM), associated with a digital camera (DLT-Cam PRO). For structures that could not be satisfactorily focused in a single light microscope photograph, a stack of 2–3 images were taken with an equidistance of ca 0.2 µm and assembled manually into a single deep-focus image in Corel Photo-Paint X6, ver. 16.4.1.1281. Specimens for scanning electron microscopy were prepared according to the protocol of Camarda *et al.* (2023). The specimens were then mounted on stubs, coated with a 10 nm layer of gold and imaged with a Hitachi UHR FE-SEM SU 8010 (10 kV, working distance 8.6–8.8 mm) at the Institute of Biology, Biotechnology and Environmental Protection (Faculty of Natural Sciences, University of Silesia in Katowice, Katowice, Poland). All figures were assembled in Figure J (Mutteter & Zinck 2013).

Table 1. List of examined samples and material for DNA, light microscopy (LM) and scanning electron microscopy (SEM). Abbreviations: A = animals; E = eggs; FG = Foggia.

Sample	Locality	Coordinates	Substrate	Date – Collector	Material examined
SE.002	Möckelmossen, Öland Island, Sweden	56°32′18.2″ N 16°27′45.3″ E	Moss on rock	15 Oct. 2006 – Reinhardt M. Kristensen	DNA (2 A), LM (69 A + 63 E), SEM (23 A + 22E)
IT.137	Monte Sant'Angelo (FG), Italy	41°42′19.5″ N 15°57′29.5″ E	Moss on rock	10 Jul. 2023 – Lucia Piemontese, Matteo Vecchi	DNA (2 A), LM (47 A + 17 E), SEM (25 A + 9 E)
JYU.S606	Monte Sant'Angelo (FG), Italy	41°43′29.4″ N 15°56′40.7″ E	Lichen on tree	22 Aug. 2020 – Lucia Piemontese	DNA (1 A)

Morphometrics and morphological nomenclature

All measurements are given in micrometers (μm). Structures were measured only if the individual or egg was in good condition and its orientation was suitable. Body length was measured from the anterior extremity to the posterior end of the body, excluding the hind legs. Buccal tube length and the level of the stylet support insertion point were measured according to Pilato (1981). The *pt* index is the ratio of the length of a given structure to the length of the buccal tube (Pilato 1981). Measurements of buccal tube widths, heights of claws and eggs, as well as the terminology used to describe the oral cavity armature (OCA) and eggshell morphology follow Guidetti *et al.* (2016) and Stec *et al.* (2020b). The common tract index (*cct*) of the claws was calculated following Guidetti *et al.* (2016). The description of the cuticular bars on the legs follows Kiosya *et al.* (2021). We measured six additional traits according to Stec *et al.* (2020b): hatchlings cuticular pore density (PD = the number of pores per 2500 μm^2 counted within a rectangle in the dorsal cuticle between legs III and IV), hatchlings pore size (PS = measured as the largest diameter; about ten pores per measured specimen), number of teeth in the external and internal lunules on the 3rd pair of claws, and number of teeth in the anterior and posterior lunules on the 4th pair of claws. Morphometric data were handled using the "Parachela" ver. 1.8 template available from the Tardigrada Register (Michalczyk & Kaczmarek 2013). The raw morphometric data are provided as Supp. files 1, 2, 3, 4. Tardigrade taxonomy follows Pilato & Binda (2010), Bertolani *et al.* (2014), Stec *et al.* (2020c, 2021) and Guidetti *et al.* (2021).

Genotyping

DNA was extracted from individual animals following a Chelex® 100 resin (BioRad) extraction method by Casquet *et al.* (2012) with modifications described in detail in Stec *et al.* (2020a). We sequenced four DNA fragments, three nuclear (18S rRNA, 28S rRNA, ITS2) and one mitochondrial (COI). All fragments were amplified and sequenced according to the protocols described in Stec *et al.* (2020c). Sequencing products were read with an ABI 3130xl sequencers at the Department of Biological and Environmental Sciences (University of Jyväskylä, Finland) and at the Institute of Systematics and Evolution of Animals (Polish Academy of Sciences, Poland).

Phylogenetic reconstruction and species delimitation analysis

The phylogenetic analyses were conducted using concatenated 18S rRNA + 28S rRNA + COI + ITS2 sequences. Only isolates with at least one COI sequence were used. The GenBank accession numbers of the newly generated sequences and those used in the phylogenetic reconstruction are presented in Table 2. As 28S rRNA sequences in GenBank mostly come from two non-overlapping fragments of the gene, they were aligned independently and considered as different partitions. The 18S rRNA, 28S rRNA, and ITS2 sequences were aligned with MAFFT ver. 7 (Katoh *et al.* 2002; Katoh & Toh 2008) with the G-INS-i method (thread = 4, threadtb = 5, threadit = 0, reorder, adjustdirection, anysymbol, maxiterate = 1000, retree 1, globalpair input). The COI sequences were aligned according to their amino

Table 2 (continued on next page). GenBank accession numbers of the sequences used in this study. In **bold:** newly generated sequences. The species/UCS attributed to the sequences in previous studies or in the results section of this study are indicated before each group of sequences.

	18S	28S-1	28S-2	COI	ITS2	References
***Richtersius nicolai* sp. nov.**						
Richtersius sp. IT.137 1				PP986909		**This study**
Richtersius sp. IT.137 2				PP986910		**This study**
Richtersius sp. JYU.S606	PP989298	PP989299		PP986911	PP989300	**This study**
Richtersius sp. C2369 1	HQ604987		KT778695	AY598780		Bertolani *et al*. 2014; Guidetti *et al.* 2005, 2016
Richtersius sp. C2369 2	HQ604988		KT778696	AY598781		Bertolani *et al*. 2014; Guidetti *et al.* 2005, 2016
***Richtersius ingemari* sp. nov.**						
Richtersius sp. SE.002 1				PP986907		**This study**
Richtersius sp. SE.002 2				PP986908		**This study**
Richtersius sp. Coro 3	AY582123			EU251385		Jørgensen & Kristensen 2004; Faurby *et al.* 2008
Richtersius sp. Sweden				EU244606		Unpublished
Richtersius sp. C3226 Rc1	KT778706		KT778697	EU251383		Guidetti *et al.* 2016; Faurby *et al.* 2008
Richtersius sp. C3226 Rc2	KT778707		KT778698	EU251384		Guidetti *et al.* 2016; Faurby *et al.* 2008
Richtersius sp. JAG.IT.120	MH681761	MH681758		MH676054	MH681764	Stec *et al.* 2020b
Richtersius sp. JAG.PL.246	MH681762	MH681759		MH676055	MH681765	Stec *et al.* 2020b
Richtersius tertius						
Richtersius tertius GR.008 1	MK211386	MK211384		MK214323	MK211380	Pogwizd & Stec 2022
Richtersius tertius GR.008 2				MK214324	MK211381	Pogwizd & Stec 2022
Richtersius tertius GR.008 3				MK214325		Pogwizd & Stec 2022
Richtersius coronifer						
Richtersius coronifer NO.385	MH681760	MH681757		MH676053	MH681763	Stec *et al.* 2020b
Richtersius coronifer Greenland				EU244607		Unpublished
Richtersius coronifer C3585 Rc1	KT778712		KT778702	KT778690		Guidetti *et al.* 2016
Richtersius coronifer C3585 Rc2	KT778713			KT778691		Guidetti *et al.* 2016
Richtersius coronifer C3585 Rc3				KT778692		Guidetti *et al.* 2016
Richtersius coronifer C3585 Rc4				KT778693		Guidetti *et al.* 2016
Richtersius coronifer C3585 V01				KT778694		Guidetti *et al.* 2016
Richtersius ziemowiti						
Richtersius ziemowiti NEP41		MT241892		MT246502		Kayastha *et al.* 2020
Richtersius ziemowiti NEP42		MT241893		MT246503		Kayastha *et al.* 2020
Richtersius ziemowiti NEP43	MT241891	MT241895		MT246504	MT241896	Kayastha *et al.* 2020
***Richtersius* sp. [Ca1 MK214326]**						
Richtersius sp. JAG.IT.317 1	MK211387	MK211385		MK214326	MK211382	Stec *et al.* 2020b
Richtersius sp. JAG.IT.317 2				MK214327	MK211383	Stec *et al.* 2020b
Richtersius sp. JAG.IT.317 3				MK214328		Stec *et al.* 2020b

Table 2 (continued). GenBank accession numbers of the sequences used in this study. In **bold:** newly generated sequences. The species/UCS attributed to the sequences in previous studies or in the results section of this study are indicated before each group of sequences.

	18S	28S-1	28S-2	COI	ITS2	References
***Richtersius* sp. [Ca2 KT778685]**						
Richtersius sp. C2595 F	KT778708		KT778699	KT778683		Guidetti *et al.* 2016
Richtersius sp. C2595 V01				KT778687		Guidetti *et al.* 2016
Richtersius sp. C2595 2F	KT778709		KT778700	KT778684		Guidetti *et al.* 2016
Richtersius sp. C2595 V02				KT778688		Guidetti *et al.* 2016
Richtersius sp. C2595 V03				KT778689		Guidetti *et al.* 2016
Richtersius sp. C2595 26	KT778710		KT778701	KT778685		Guidetti *et al.* 2016
Richtersius sp. C2595 2M				KT778686		Guidetti *et al.* 2016
***Richtersius* sp. [Ca3 GU237485]**						
Richtersius sp. TW 1				GU237485		Unpublished
Richtersius sp. TW 2				GU339056		Unpublished
Outgroups						
Diaforobiotus hyperonyx	OM179854	OM179862		OM151289	OM179869	Stec & Morek 2022
Diaforobiotus islandicus	MT812470	MT812461		MT808072	MT812597	Stec *et al.* 2020c
Diaforobiotus svalbardicus	MT812471	MT812463		MT808074	MT812598	Stec *et al.* 2020c

acid sequences (translated using the invertebrate mitochondrial code) with the MUSCLE algorithm (Edgar 2004) in MEGA7 with default settings (all gap penalties = 0, max iterations = 8, clustering method = UPGMB, lambda = 24). Alignments were visually inspected and trimmed in MEGA7. Sequences were concatenated with the R package 'concatipede' ver. 1.0.0 (Vecchi & Bruneaux 2021). Model selection was performed for each alignment partition (6 in total: 18S rRNA, 28S rRNA, ITS2 and three COI codons) using PartitionFinder2 (Lanfear *et al.* 2017). Bayesian inference (BI) phylogenetic reconstruction was performed using MrBayes ver. 3.2.6 (Ronquist *et al.* 2012) without BEAGLE. Two runs (one cold chain and three heated chains each) of 20 million generations were used with a burn-in of 2 million generations, sampling a tree every 1000 generations. ESS and sanity of the posteriors were checked with Tracer ver. 1.6 (available from https://github.com/beast-dev/tracer). The consensus tree was visualized in FigTree ver. 1.4.3 (available from http://tree.bio.ed.ac.uk/software/figtree). The MrBayes input file is available as Supp. file 5.

ASAP species delimitation was performed on the COI alignment on the ASAP online server (Puillandre *et al.* 2021) using JC69 distance and default parameters (complete results are available as Supp. file 6).

Results

The phylogenetic analysis recovered 8 monophyletic clades in *Richtersius* that were also confirmed by the ASAP species delimitation as separate putative species (Fig. 1). Three species are already formally described (*R. coronifer*, *R. ziemowiti*, *R. tertius*). For two more putative species enough morphological and physiological differences were identified to allow their formal description (see Taxonomic account). For three more putative species there is no morphological data available to formally describe them and are identified as Unconfirmed Candidate Species (UCS; Padial *et al.* 2010) (see Taxonomic account).

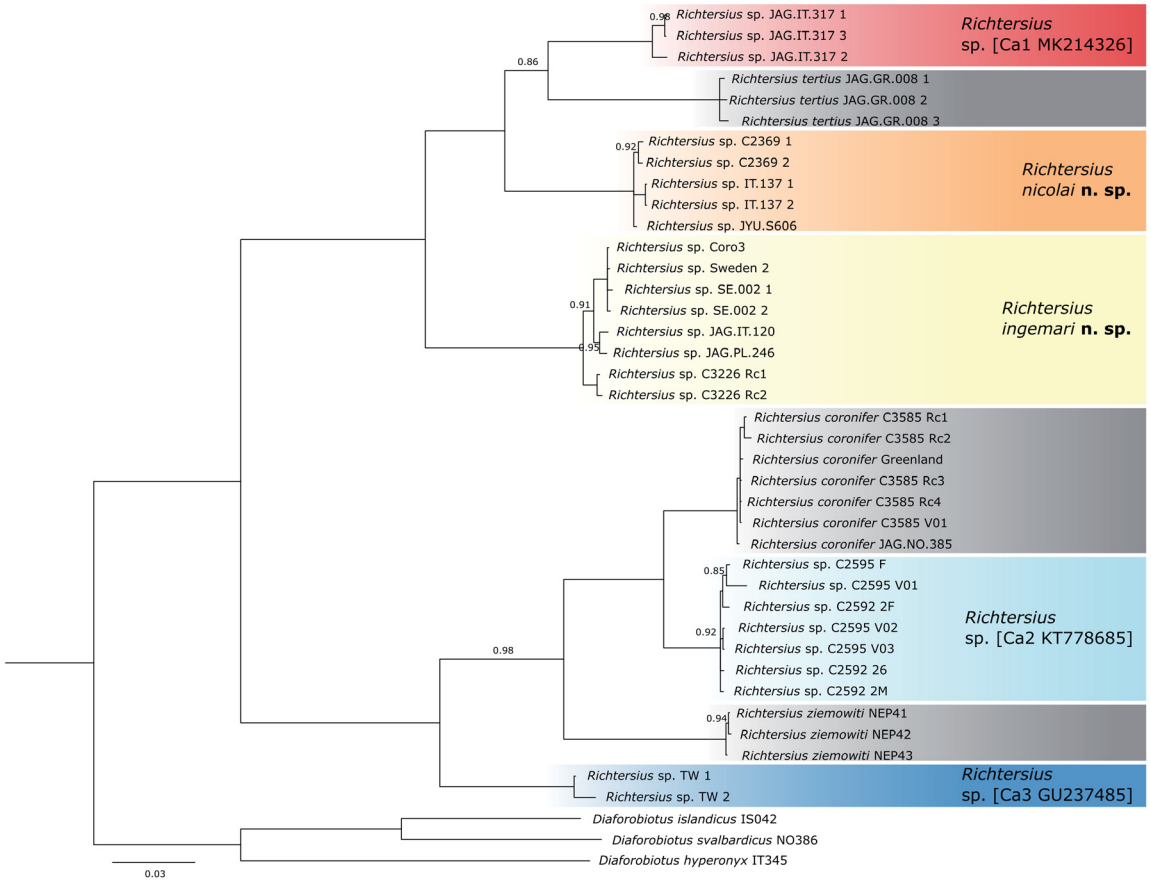

Fig. 1. Phylogenetic reconstruction of the genus *Richtersius* Pilato & Binda, 1989 obtained with Bayesian Inference. Numbers above branches indicate posterior probability (pp). When pp = 1, support is not indicated. Nodes with pp = 0.70 were collapsed. Shaded boxes represent species identified by ASAP analysis based on the COI alignment.

Taxonomic account

Phylum Tardigrada Doyère, 1840
Class Eutardigrada Richters, 1926
Order Macrobiotoidea Thulin, 1928
Family Richtersiusidae Guidetti, Schill, Giovannini, Massa, Goldoni, Ebel, Förschler, Rebecchi, Cesari, 2021
Genus ***Richtersius*** Pilato & Binda, 1989

Richtersius nicolai sp. nov.
urn:lsid:zoobank.org:act:1BC3E5B8-7DB4-4BC0-BBD9-820FD28BFECD
Figs 2–7; Tables 3–5

Richtersius coronifer – Guidetti *et al.* 2005.
Richtersius Northern Italy 1 – Guidetti *et al.* 2016: fig. 1.
Richtersius sp. 5 – Stec *et al.* 2020b.
Richtersius aff. *coronifer* – Zawierucha *et al.* 2023.

Etymology

This species is named after Nicola Piemontese, a naturalist and expert of the flora and fauna of the Gargano Peninsula.

Type material

Holotype

ITALY • Monte Sant'Angelo; 41°42′19.5″ N, 15°57′29.5″ E; 790 m a.s.l.; Jul. 2023; M. Vecchi and L. Piemontese leg.; moss on rock; ISEA-PAS, slide IT.137.4.

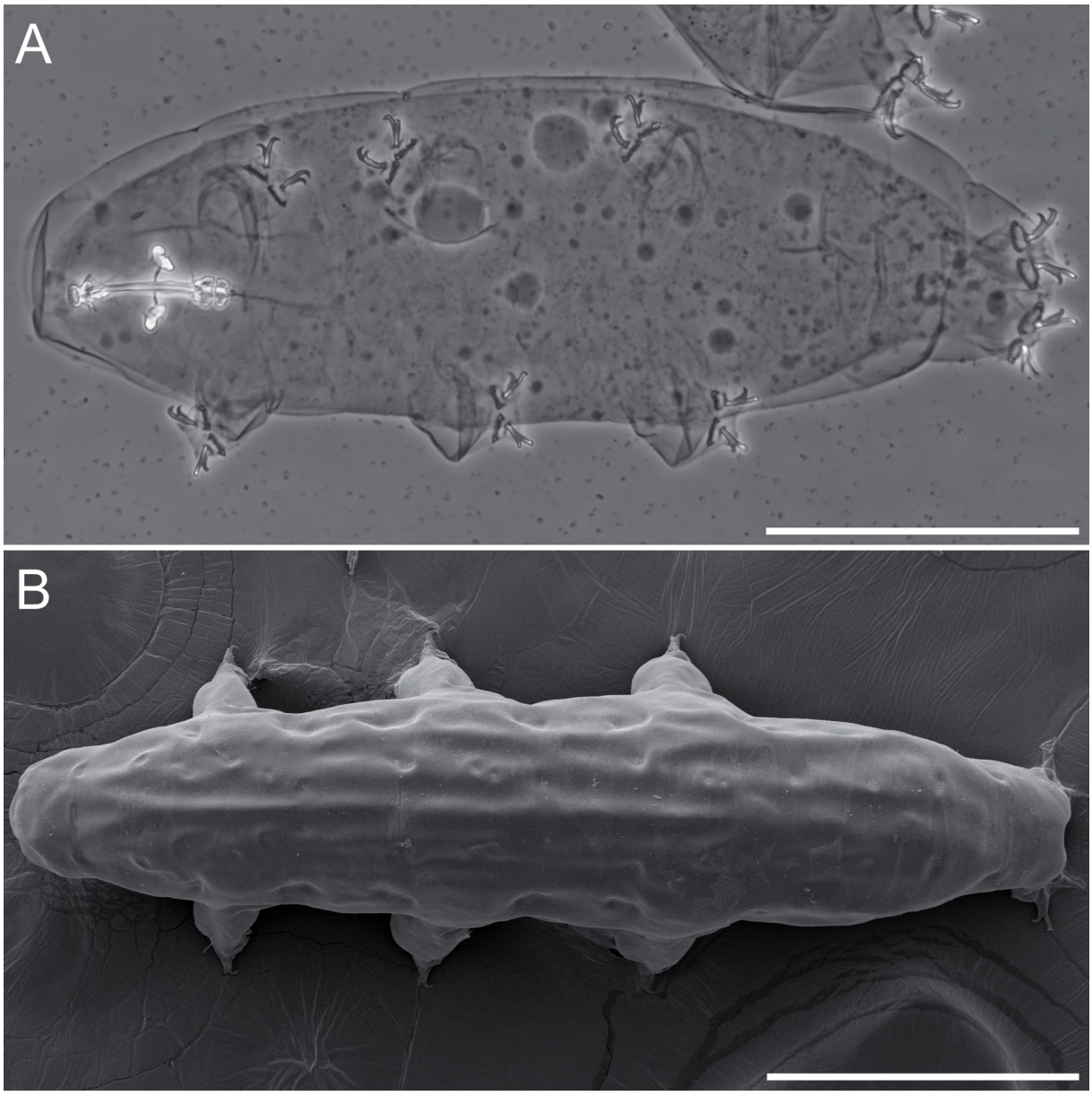

Fig. 2. Adult *Richtersius nicolai* sp. nov. from sample IT.137 (holotype and paratype ISEA-PAS), habitus. **A**. Holotype habitus (PCM). **B**. Paratype habitus (SEM). Scale bars = 200 µm.

Paratypes

ITALY • 60 specs; same data as for holotype; ISEA PAS, slides IT.137.1 to IT.137.6 and slides IT.137.10 to IT.137.13, SEM stubs TAR.2.03, TAR.2.04 • 12 eggs; same data as for holotype; ISEA PAS, slide IT.137.8, SEM stub TAR.2.05 • 5 specs; same data as for holotype; MUC, slide NHMD-1732285 • 6 eggs; same data as for holotype; MUC, slide NHMD-1732286.

Description

Animals (measurements in Tables 3–4; Supp. files 1, 2)

Body is bright yellow; all specimens became transparent after the fixation in Hoyers's medium (Fig. 2). Eyes were visible in 64% of animals (excluding hatchlings) mounted in Hoyers's medium. Body and leg cuticle is without granulation in all life stages and with pores present only in hatchlings (Fig. 3).

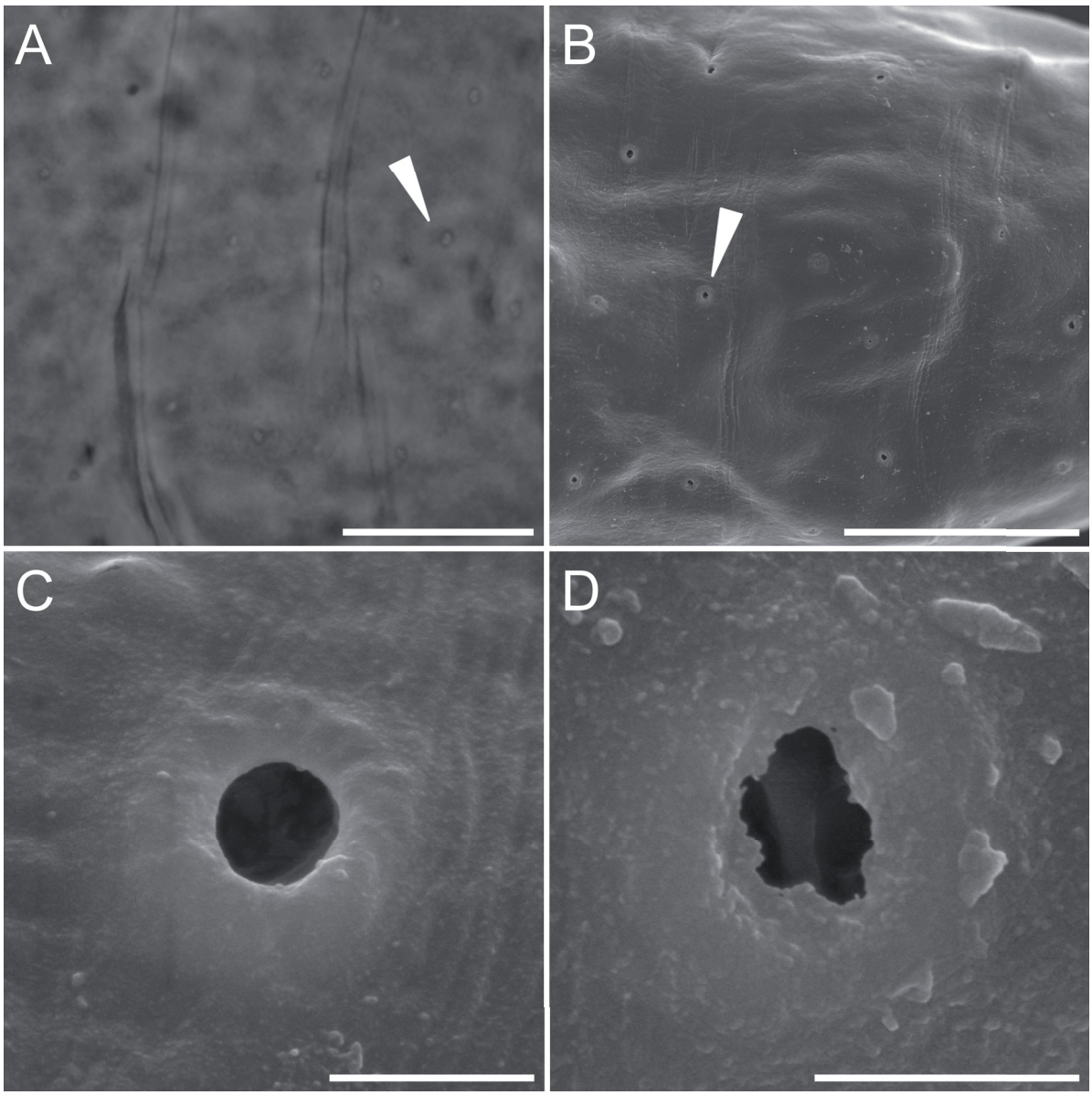

Fig. 3. Newborn *Richtersius nicolai* sp. nov. from sample IT.137 (paratypes ISEA-PAS), cuticular pores in newborns. **A**. Dorso-caudal cuticle with pores (PCM). **B**. Dorso-caudal cuticle with pores (SEM). **C–D**. Pores (SEM). Arrowheads indicate pores on the cuticle. Scale bars: A–B = 20 μm; C–D = 1 μm.

Table 3 (continued on next page). Measurements (in µm) and *pt* values of selected morphological structures of adults of *Richtersius nicolai* sp. nov. excluding hatchlings. Specimens mounted in Hoyer's medium. Range refers to the smallest and the largest structure among all measured specimens. Abbreviations: N = number of specimens/structures measured; SD = standard deviation.

Character	N	Range		Mean		SD		Holotype	
		µm	*pt*	µm	*pt*	µm	*pt*	µm	*pt*
Body length	14	493–853	*740–1171*	640	*910*	104	*119*	634	*920*
Buccal tube									
Buccal tube length	14	58.0–76.5		70.2		5.3		68.9	
Stylet support insertion point	10	40.8–52.9	67.6–71.1	48.3	70.0	4.0	1.2	48.3	*70.1*
Buccal tube external width	14	4.2–5.3	*5.8–7.7*	4.7	*6.7*	0.3	*0.6*	5.3	*7.7*
Buccal tube internal width	14	1.4–3.0	*2.1–4.3*	2.1	*3.1*	0.5	*0.7*	1.8	*2.6*
Ventral lamina length	13	23.1–35.3	*34.7–48.9*	30.0	*43.0*	4.3	*5.1*	26.5	*38.5*
Placoid lengths									
Macroplacoid 1	12	6.2–9.6	*10.2–13.8*	8.1	*11.6*	1.0	*1.1*	8.1	*11.7*
Macroplacoid 2	14	6.2–8.2	*9.3–13.4*	7.4	*10.6*	0.6	*1.0*	6.5	*9.5*
Placoid row	14	14.6–22.5	*22.3–31.0*	17.8	*25.5*	2.0	*2.8*	16.7	*24.2*
Claw I heights									
External base	12	8.7–15.0	*12.2–20.6*	11.5	*16.4*	1.7	*2.2*	11.0	*16.0*
External primary branch	13	15.2–24.9	*25.7–34.1*	20.6	*29.3*	2.8	*2.8*	19.7	*28.6*
External secondary branch	13	12.1–20.0	*19.6–27.5*	16.3	*23.2*	2.4	*2.7*	15.8	*22.9*
External base/primary branch (*cct*)	12	46.3–61.1		55.8		4.6		56.0	
Internal base	11	8.8–14.1	*14.5–18.4*	11.6	*16.7*	1.6	*1.5*	12.2	*17.7*
Internal primary branch	13	15.5–24.3	*24.8–32.8*	19.9	*28.4*	2.7	*2.5*	19.7	*28.6*
Internal secondary branch	13	11.6–20.4	*19.6–28.1*	16.1	*23.0*	2.5	*2.7*	16.1	*23.3*
Internal base/primary branch (*cct*)	11	49.3–64.2		58.1		3.9		61.9	
Claw II heights									
External base	12	8.5–16.0	*13.1–21.9*	12.3	*17.5*	2.4	*2.7*	11.4	*16.5*
External primary branch	13	16.0–25.4	*24.3–34.9*	21.0	*30.0*	3.2	*3.5*	22.0	*31.9*
External secondary branch	13	12.5–20.8	*18.0–28.6*	16.8	*24.0*	2.8	*3.2*	16.9	*24.5*
External base/primary branch (*cct*)	12	51.6–63.0		57.5		3.9		51.6	
Internal base	11	9.2–15.2	*13.8–20.8*	11.9	*17.0*	2.0	*2.4*	11.4	*16.6*
Internal primary branch	13	15.0–25.1	*24.1–33.0*	20.2	*28.8*	3.1	*3.0*	20.5	*29.7*
Internal secondary branch	13	10.9–21.3	*15.7–29.2*	16.6	*23.6*	3.1	*3.6*	16.3	*23.6*
Internal base/primary branch (*cct*)	11	47.1–63.9		57.4		5.1		55.9	
Claw III heights									
External base	13	7.8–16.7	*13.5–23.1*	12.6	*17.9*	2.5	*3.0*	11.7	*17.0*
External primary branch	13	15.3–26.2	*26.3–36.0*	21.5	*30.6*	3.0	*2.8*	20.5	*29.7*
External secondary branch	13	11.9–26.6	*20.6–35.8*	18.3	*26.0*	3.5	*4.0*	16.6	*24.1*
External base/primary branch (*cct*)	13	50.6–69.3		58.4		5.5		57.3	
Internal base	11	8.3–15.0	*12.1–20.7*	12.0	*17.1*	1.8	*2.5*	8.3	*12.1*
Internal primary branch	13	13.3–26.5	*23.0–34.6*	20.6	*29.3*	3.4	*3.5*	17.3	*25.1*
Internal secondary branch	12	13.0–20.6	*18.8–28.0*	17.2	*24.3*	2.2	*2.6*	13.0	*18.8*
Internal base/primary branch (*cct*)	11	48.1–66.2		57.6		5.7		48.1	

Table 3 (continued). Measurements (in µm) and *pt* values of selected morphological structures of adults of *Richtersius nicolai* sp. nov. excluding hatchlings. Specimens mounted in Hoyer's medium. Range refers to the smallest and the largest structure among all measured specimens. Abbreviations: N = number of specimens/structures measured; SD = standard deviation.

Character	N	Range		Mean		SD		Holotype	
		µm	*pt*	µm	*pt*	µm	*pt*	µm	*pt*
Claw IV heights									
Anterior base	13	11.7–18.5	*17.3–25.3*	14.9	*21.3*	2.2	*2.4*	15.6	*22.7*
Anterior primary branch	13	20.8–33.0	*30.5–44.8*	27.1	*38.7*	4.2	*4.9*	26.9	*39.0*
Anterior secondary branch	13	14.7–24.7	*21.2–34.1*	19.8	*28.3*	3.3	*3.7*	19.7	*28.5*
Anterior base/primary branch (*cct*)	13	49.3–63.2		55.5		4.8		58.2	
Posterior base	12	11.2–20.1	*18.6–27.6*	15.5	*22.1*	2.9	*3.0*	15.2	*22.1*
Posterior primary branch	13	20.6–35.2	*31.4–48.4*	27.2	*38.8*	4.5	*4.7*	27.0	*39.1*
Posterior secondary branch	12	10.7–28.0	*15.5–38.4*	20.2	*28.7*	4.7	*5.6*	10.7	*15.5*
Posterior base/primary branch (*cct*)	12	49.4–64.5		56.0		3.9		56.4	
Number of teeth on internal lunula III	12	8–12		9.9		1.4		9	
Number of teeth on external lunula III	10	8–13		9.7		1.5		10	
Number of teeth on anterior lunula IV	11	7–14		10.5		2.3		13	
Number of teeth on posterior lunula IV	10	8–18		13.7		3.0			

Hatchlings are similar in appearance to adults, except for a smaller body size and roundish pores (Fig. 3) (1.14–2.10 µm in diameter) with sometimes jagged edges, faintly visible under PCM, scattered randomly throughout the body cuticle, with a mean pore density of 10 (range 9–11) per 2500 µm^2 of the dorsal cuticle.

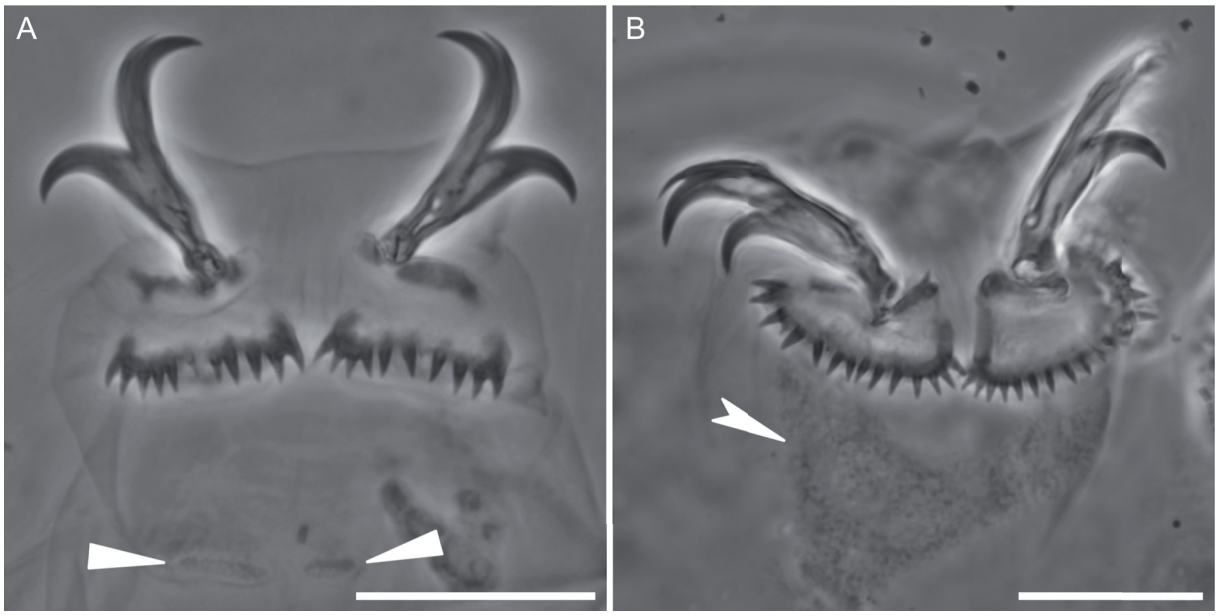

Fig. 4. Adult *Richtersius nicolai* sp. nov. from sample IT.137 (paratypes ISEA-PAS), claws and associated structures. **A**. Claws I (PCM). **B**. Claws IV (PCM). Arrowheads indicate muscle attachments. Indented arrowhead indicates horseshoe structure under claws IV. Scale bars = 20 µm.

Claws are slender, primary branches with distinct accessory points (Fig. 4) and an internal system of septa as described for *Richtersius coronifer* s. lat. by Lisi *et al.* (2020). The claw common tract index has an average value between 56% and 58% across all four leg pairs, meaning that the basal portion of the claw is usually longer than half the total length of the primary branch. Lunulae are large, with a crown of long, numerous and densely arranged spikes (Fig. 4). All the lunulae are trapezoidal (Fig. 4). Double muscle attachments in legs I–III and horseshoe structures in legs IV are visible in PCM, whereas cuticular bars are absent (Fig. 4).

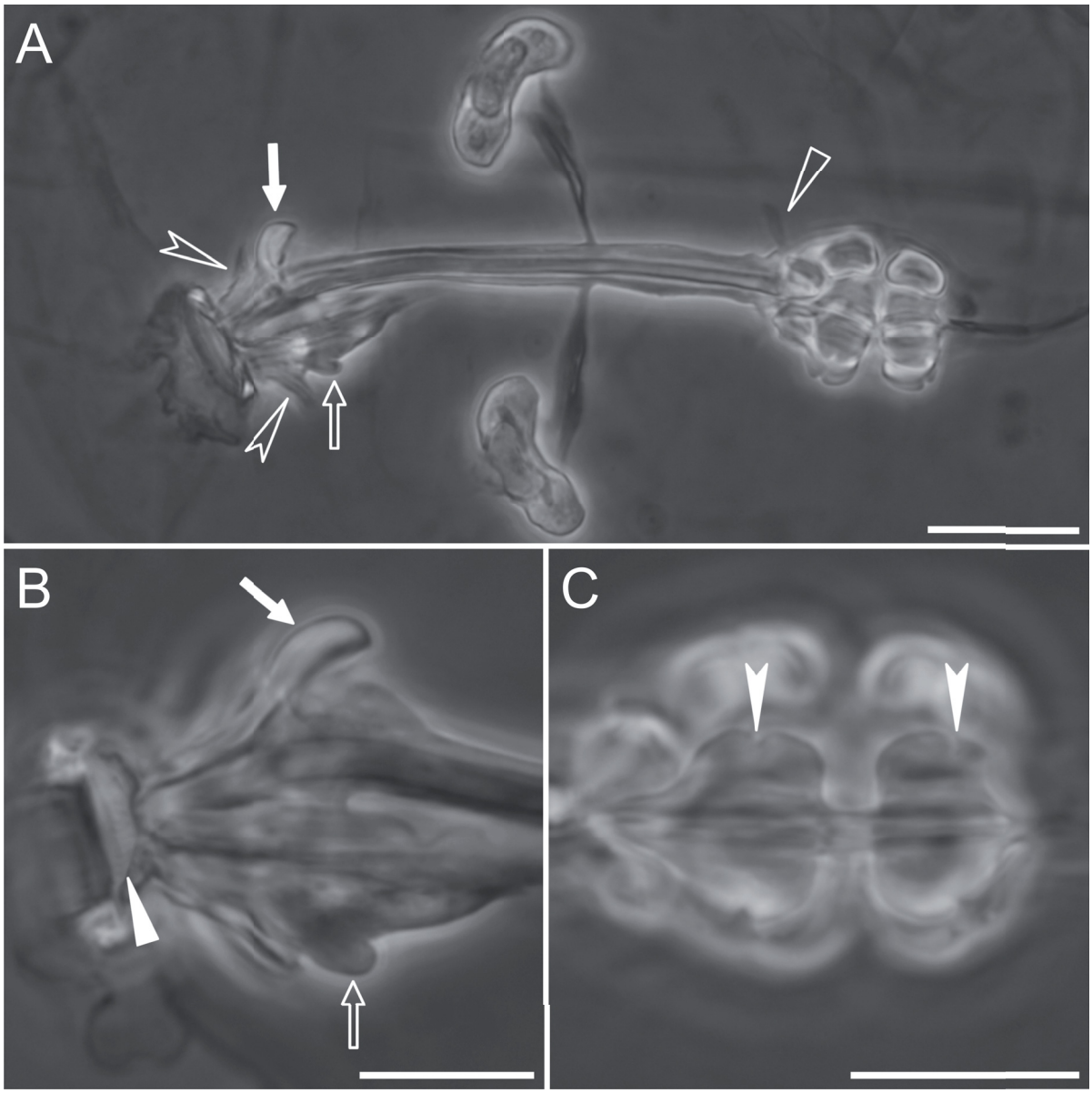

Fig. 5. Adult *Richtersius nicolai* sp. nov. from sample IT.137 (paratypes ISEA-PAS), buccal apparatus. **A**. Entire buccal apparatus (PCM). **B**. Lateral view of the buccal crown (PCM). **C**. Macroplacoids (PCM). Filled arrows indicate dorsal hook of the apophyses for the insertion of the stylet muscles (AISM). Empty arrows indicate ventral hook of AISM. Empty indented arrowheads indicate triangular apophyses of the buccal crown. Empty arrowhead indicates anterior cuticular spike. Filled arrowhead indicates the third OCA ring. Filled indented arrowheads indicate placoids constrictions. Scale bars: A = 20 μm; B–C = 10 μm.

Mouth is antero-ventral. The buccal apparatus is of the *Richtersius* type (Fig. 5). The oral cavity is followed by a system of large apophyses that form a buccal crown (Fig. 5A–B). Anteriorly, the system consists of dorso-lateral and ventro-lateral triangular apophyses (Fig. 5A). The dorsal and ventral apophyses are composed of anteriorly positioned large cuticular hooks, followed by longitudinal crests (Fig. 5B). The hook in the ventral apophyses is smaller than the dorsal hook (Fig. 5B). The wall of the buccal tube exhibits a variable thickness (Fig. 5A), but the internal diameter of the buccal tube is almost uniformly narrow (Fig. 5A). From the mouth opening to the stylet support insertion point, the thickness of the buccal tube wall increases only slightly, while below this point the evident posterior thickness is clearly visible (Fig. 5A). The pharynx is spherical, with bilobed apophyses, three anterior cuticular spikes (typically only two are visible in any given plane) and two granular macroplacoids (2 < 1).

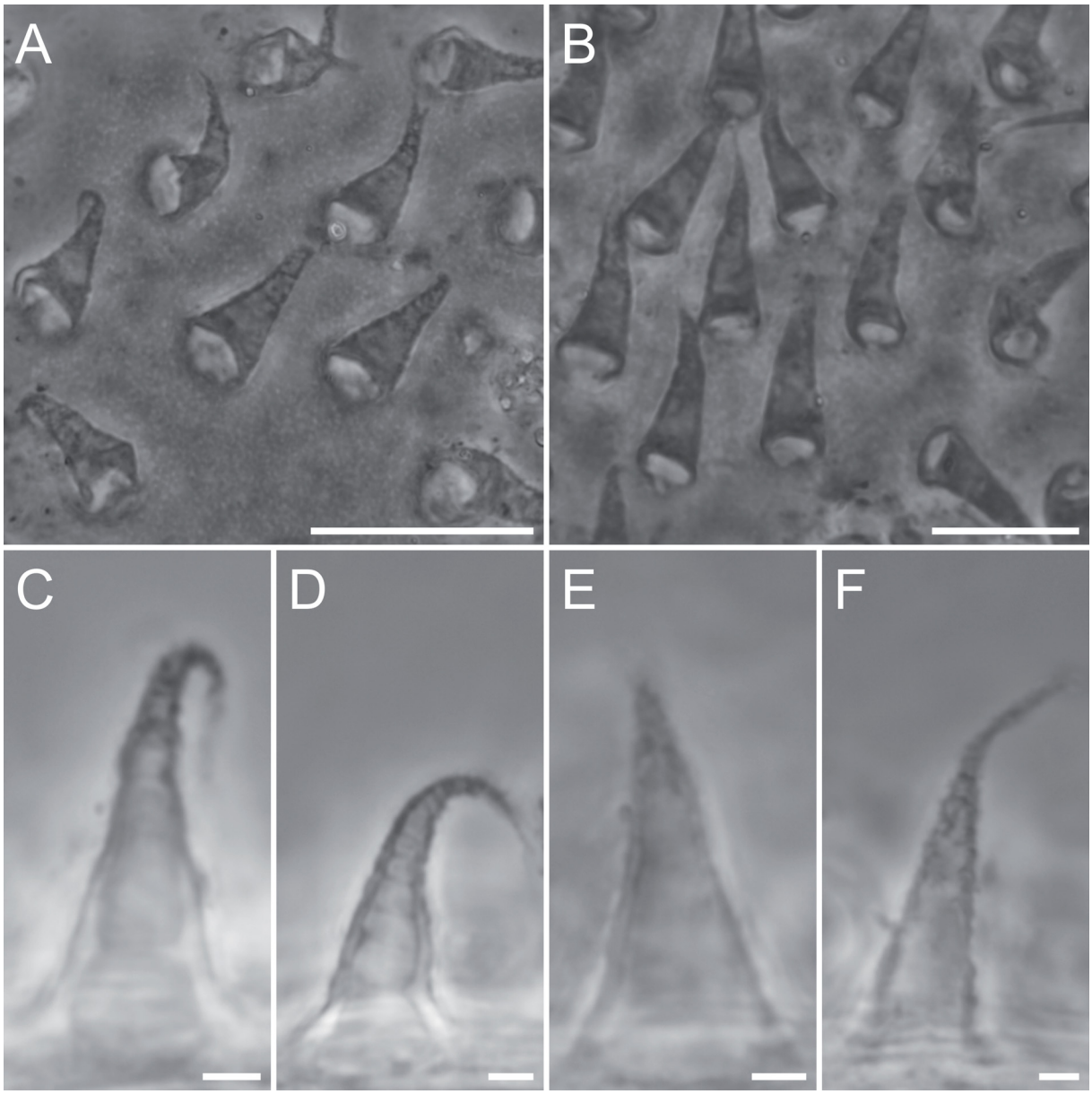

Fig. 6. Eggs of *Richtersius nicolai* sp. nov. from sample IT.137 (paratypes ISEA-PAS). **A–B**. Chorion surface and processes (PCM). **C–F**. Egg processes (PCM). Scale bars: A = 20 μm; B = 10 μm; C–F = 2 μm.

Table 4 (continued on next page). Measurements (in µm) and *pt* values of selected morphological structures of hatchlings of *Richtersius nicolai* sp. nov. Specimens mounted in Hoyer's medium. Range refers to the smallest and the largest structure among all measured specimens. Abbreviations: N = number of specimens/structures measured; SD = standard deviation.

Character	N	Range		Mean		SD	
		µm	*pt*	µm	*pt*	µm	*pt*
Body length	5	294 – 359	*526 – 653*	330	*608*	25	*53*
Buccal tube							
Buccal tube length	6	52.2 – 55.9		54.4		1.5	
Stylet support insertion point	5	37.3 – 38.2	*67.8 – 71.3*	37.8	*69.8*	0.4	*1.3*
Buccal tube external width	6	3.5 – 4.2	*6.2 – 7.7*	3.8	*7.0*	0.3	*0.6*
Buccal tube internal width	6	1.1 – 1.7	*2.1 – 3.2*	1.4	*2.6*	0.2	*0.4*
Ventral lamina length	3	20.5 – 27.3	*38.5 – 48.8*	23.4	*42.7*	3.5	*5.4*
Placoid lengths							
Macroplacoid 1	6	5.8 – 7.3	*10.4 – 13.7*	6.2	*11.5*	0.6	*1.2*
Macroplacoid 2	6	4.8 – 6.6	*8.6 – 12.3*	5.7	*10.4*	0.6	*1.3*
Placoid row	6	12.2 – 15.5	*21.8 – 29.1*	13.2	*24.3*	1.2	*2.6*
Claw I heights							
External base	5	6.8 – 8.4	*12.5 – 16.0*	7.5	*13.9*	0.8	*1.8*
External primary branch	5	12.4 – 15.1	*22.7 – 29.0*	13.7	*25.4*	1.1	*2.4*
External secondary branch	5	9.4 – 10.7	*16.9 – 20.4*	9.9	*18.3*	0.5	*1.3*
External base/primary branch (*cct*)	5	48.2 – 64.0		54.9		5.8	
Internal base	5	5.8 – 7.8	*10.7 – 14.9*	6.9	*12.8*	0.7	*1.6*
Internal primary branch	5	11.9 – 14.8	*21.8 – 27.0*	13.0	*24.0*	1.1	*2.1*
Internal secondary branch	5	9.2 – 11.5	*16.7 – 21.0*	9.9	*18.4*	1.0	*2.0*
Internal base/primary branch (*cct*)	5	49.0 – 60.0		53.5		4.5	
Claw II heights							
External base	4	6.3 – 9.9	*11.6 – 18.5*	8.3	*15.2*	1.6	*3.0*
External primary branch	4	13.5 – 14.6	*24.8 – 27.5*	14.2	*26.0*	0.5	*1.2*
External secondary branch	4	9.8 – 11.3	*17.7 – 21.2*	10.3	*18.8*	0.7	*1.6*
External base/primary branch (*cct*)	4	43.7 – 67.4		58.4		10.7	
Internal base	3	6.5 – 9.1	*11.9 – 16.7*	8.2	*15.0*	1.4	*2.7*
Internal primary branch	3	13.2 – 14.0	*24.8 – 25.4*	13.7	*25.1*	0.4	*0.3*
Internal secondary branch	3	9.9 – 10.6	*18.4 – 19.4*	10.3	*18.8*	0.3	*0.5*
Internal base/primary branch (*cct*)	3	46.9 – 67.2		59.7		11.2	
Claw III heights							
External base	4	7.9 – 9.0	*14.5 – 16.9*	8.6	*15.9*	0.5	*1.0*
External primary branch	4	13.0 – 14.3	*23.3 – 26.8*	13.6	*25.3*	0.6	*1.8*
External secondary branch	4	10.2 – 10.5	*18.2 – 19.7*	10.3	*19.2*	0.1	*0.7*
External base/primary branch (*cct*)	4	59.8 – 69.1		63.0		4.4	
Internal base	4	7.1 – 7.8	*12.8 – 15.0*	7.6	*14.1*	0.3	*1.0*
Internal primary branch	4	11.8 – 13.4	*21.0 – 25.2*	12.6	*23.4*	0.7	*1.7*
Internal secondary branch	4	8.3 – 10.8	*14.9 – 19.9*	9.7	*18.1*	1.1	*2.2*
Internal base/primary branch (*cct*)	4	57.2 – 63.5		60.3		2.6	

Table 4 (continued). Measurements (in µm) and *pt* values of selected morphological structures of hatchlings of *Richtersius nicolai* sp. nov. Specimens mounted in Hoyer's medium. Range refers to the smallest and the largest structure among all measured specimens. Abbreviations: N = number of specimens/structures measured; SD = standard deviation.

Character	N	Range		Mean		SD	
		µm	*pt*	µm	*pt*	µm	*pt*
Claw IV heights							
Anterior base	4	8.9 – 11.4	*15.9 – 21.3*	10.0	*18.5*	1.1	*2.5*
Anterior primary branch	4	16.6 – 19.0	*29.7 – 35.8*	17.9	*33.2*	1.1	*2.9*
Anterior secondary branch	4	12.0 – 13.1	*21.9 – 24.6*	12.4	*23.0*	0.5	*1.3*
Anterior base/primary branch (*cct*)	4	52.8 – 59.6		55.6		3.1	
Posterior base	4	7.7 – 10.4	*14.0 – 19.0*	9.3	*17.2*	1.3	*2.3*
Posterior primary branch	4	16.0 – 18.7	*29.9 – 33.5*	16.9	*31.3*	1.2	*1.7*
Posterior secondary branch	4	11.1 – 13.4	*21.2 – 24.0*	11.9	*22.0*	1.0	*1.3*
Posterior base/primary branch (*cct*)	4	47.0 – 63.6		55.1		6.8	
Number of teeth on internal lunula III	5	11 – 14		12.4		1.5	
Number of teeth on external lunula III	5	9 – 16		12.2		2.6	
Number of teeth on anterior lunula IV	4	11 – 12		11.8		0.5	
Number of teeth on posterior lunula IV	4	8 – 23		14.5		6.4	
Pore density (PD)	5	9 – 11		10.2		0.8	
Pore size	49	0.9 – 2.1		1.4		0.3	

The first and second macroplacoids have a faint constriction positioned centrally and subterminally, respectively (Fig. 5C). The oral cavity armature is faintly visible under PCM, with only the second band of teeth visible mainly in the larger specimens (Fig. 5B). Under PCM, the second band of teeth is visible as several irregular rows of densely packed and faint dark dots (Fig. 5B). The discontinuous third band of teeth is situated between the second band of teeth and the opening of the buccal tube and is divided into a dorsal and a ventral portion, both in the form of a single large tooth resembling a beak.

Eggs (measurements in Table 5; Supp. file 1)

Large, roundish, yellow, laid freely. The surface between processes is smooth but with refracting dots faintly visible only under PCM, but difficult to observe because of the amount of debris that is typically attached to the egg surface (Figs 6–7). Processes in the shape of elongated, thin cones with a ragged surface caused by small granules visible both in LM and SEM (Figs 6, 7B–E). Terminal discs or other structures absent.

Reproduction

The species is gonochoric-amphimictic (Guidetti *et al.* 2016).

DNA sequences

– 18S: HQ604987–8 (Bertolani *et al.* 2014), PP989298 (this study)
– 28S: KT778695–6 (Guidetti *et al.* 2016), PP989299 (this study)
– COI: AY598780–1 (Guidetti *et al.* 2005), PP986909-11 (this study)
– ITS2: PP989300 (this study)

Distribution

Locus typicus: Monte Sant'Angelo, Puglia, Italy (41°42′19.5″ N, 15°57′29.5″ E; 790 m above sea level (a.s.l.)). Moss on rock (sample IT.137 in this study).

Monte Sant'Angelo, Puglia, Italy (41°43′29.4″ N, 15°56′40.7″ E; 800 m a.s.l.). Lichen on tree (sample JYU.S606 in this study).

Pratignano, Emilia Romagna, Italy (4°09′11.8″ N, 10°48′24.9″ E; 1500 m a.s.l.). Moss on rock (*Richtersius* Northern Italy 1 in Guidetti *et al.* 2016).

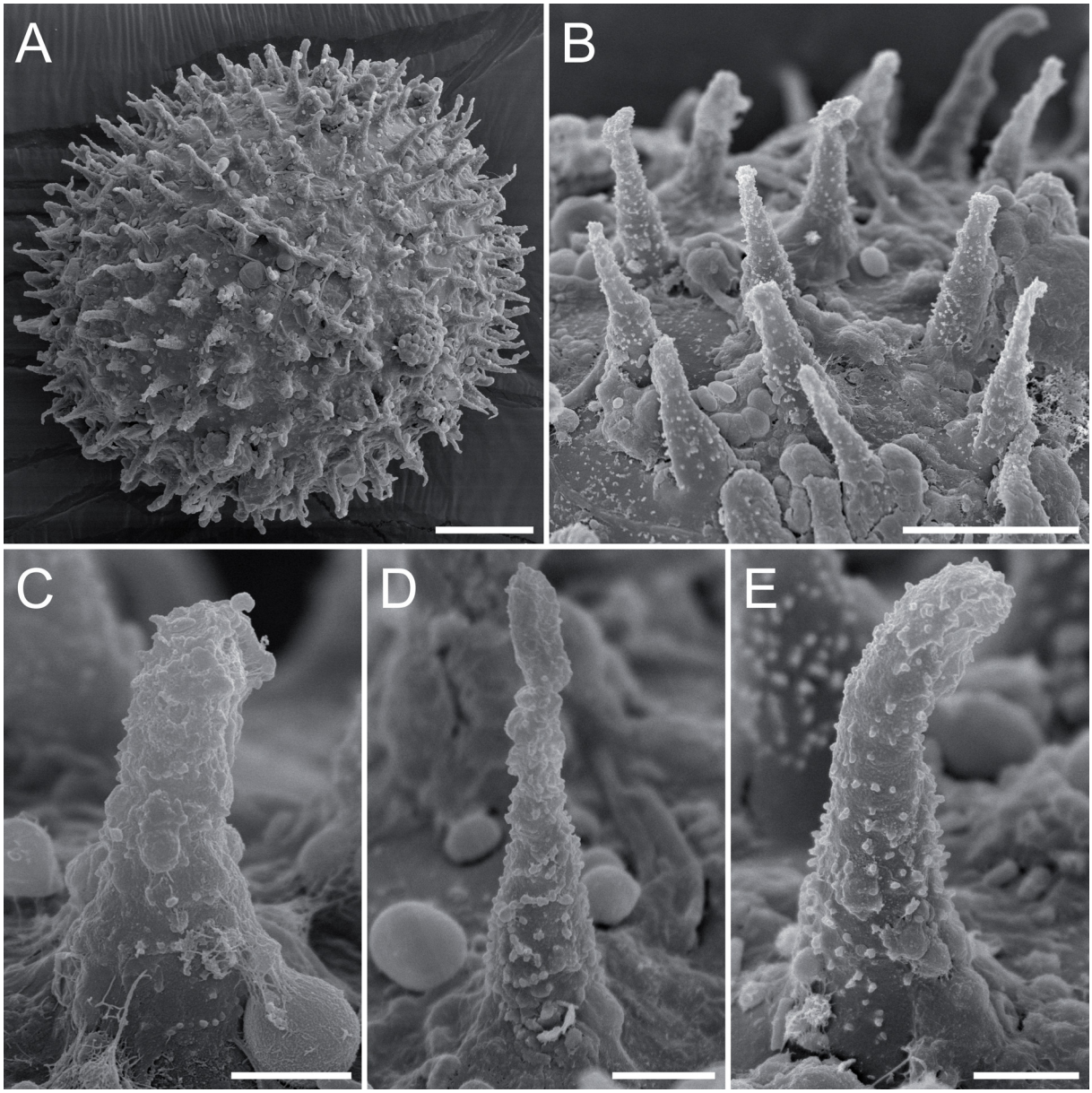

Fig. 7. Eggs of *Richtersius nicolai* sp. nov. from sample IT.137 (paratypes ISEA-PAS). **A**. Egg in toto (SEM). **B**. Chorion surface and processes (SEM). **C–E**. Egg processes (SEM). Scale bars: A = 20 µm; B = 10 µm; C–E = 2 µm.

Table 5. Measurements (in µm) of the eggs of *Richtersius nicolai* sp. nov. Eggs mounted in Hoyer's medium; process base/height ratio is expressed as percentage. Range refers to the smallest and the largest structure among all measured specimens. Abbreviations: N = number of eggs/structures measured; SD = standard deviation.

Character	N	Range	Mean	SD
Egg bare diameter	13	118.1–134.3	126.9	5.0
Egg full diameter	13	135.5–157.8	148.4	7.3
Process height	48	10.1–19.1	14.1	2.1
Process base width	48	3.1–7.3	5.3	1.1
Process base/height ratio	48	25%–54%	38%	7%
Inter-process distance	48	4.6–10.1	6.9	1.3
Number of processes on the egg circumference	13	25–38	32.1	3.4

Differential diagnosis

Richtersius nicolai sp. nov. differs from:

Richtersius coronifer by having smaller eggs (bare diameter 118–134 µm in *R. nicolai* sp. nov. vs 173–233 µm in *R. coronifer*) and by having a lower pores density in the newborns (PD 9–11 in *R. nicolai* vs 60–88 in *R. coronifer*).

Richtersius ziemowiti by having a lower pores density in the newborns (PD 9–11 in *R. nicolai* sp. nov. vs 20–24 in *R. ziemowiti*).

Richtersius mazepi by having bigger eggs (bare diameter 118–137 µm in *R. nicolai* sp. nov. vs 77–91 µm in *R. mazepi*), by the absence of a crown of thickenings distributed around the bases of the egg processes (present in *R. mazepi*), by the different shape of the egg processes (conical spikes in *R. nicolai* vs wide dome-shaped proximal portion and an elongated slender distal portion in *R. mazepi*), by having a lower pore density in the newborns (PD 9–11 in *R. nicolai* vs 26–36 in *R. mazepi*), and by having a higher claw IV anterior *cct* (*49–63* % in *R. nicolai* vs *32–44* % in *R. mazepi*).

Richtersius tertius by having a higher pore density in the newborns (PD 9–11 in *R. nicolai* sp. nov. vs 3–6 in *R. tertius*), and by having a smaller first macroplacoid (*pt = 10–14* in *R. nicolai* vs *pt = 14–20* in *R. tertius*).

Richtersius ingemari sp. nov. by having a higher pore density in the newborns (PD 9–11 in *R. nicolai* sp. nov. vs 4–7 in *R. ingemari*), and by the reproductive mode (gonochorism in *R. nicolai* vs parthenogenesis in *R. ingemari*).

Richtersius ingemari sp. nov.
urn:lsid:zoobank.org:act:8D3E6F1C-BCFA-46A6-9F5C-173C0EB70EF2
Figs 8–13; Tables 6–8

Adorybiotus coronifer – Westh & Ramløv 1991. — Ramløv & Westh 1992. — Westh & Kristensen 1992.

Adorybiotus (*Richtersius*) *coronifer* – Ramløv & Westh 2001.

Richtersius coronifer – Jönsson & Guidetti 2001. — Jönsson & Rebecchi 2002. — Ivarsson & Jönsson 2004. — Jönsson *et al.* 2005. — Jönsson 2007. — Jönsson & Schill 2007. — Dunn *et al*. 2008. — Faurby *et al.* 2008. — Hindborg Mortensen *et al.* 2010. — Nilsson *et al.* 2010. — Persson *et al.* 2011.

— Halberg *et al.* 2012; 2013. — Czernekova & Jönsson 2016. — Czerneková *et al.* 2017; 2018. — Vecchi *et al*. 2018. — Guidetti *et al.* 2019. — Kamilari *et al.* 2019. — Pedersen *et al.* 2020; 2021.
Richtersius coronifer P3 – Rebecchi *et al.* 2003.
Richtersius coronifer P4 – Rebecchi *et al.* 2003.
Richtersius Sweden – Guidetti *et al.* 2016: figs 1–2.
Richtersius Northern Italy 2 – Guidetti *et al.* 2016.
Richtersius sp. 4 – Stec *et al.* 2020b.
Richtersius cf. *coronifer* – Hagelbäck & Jönsson 2023.

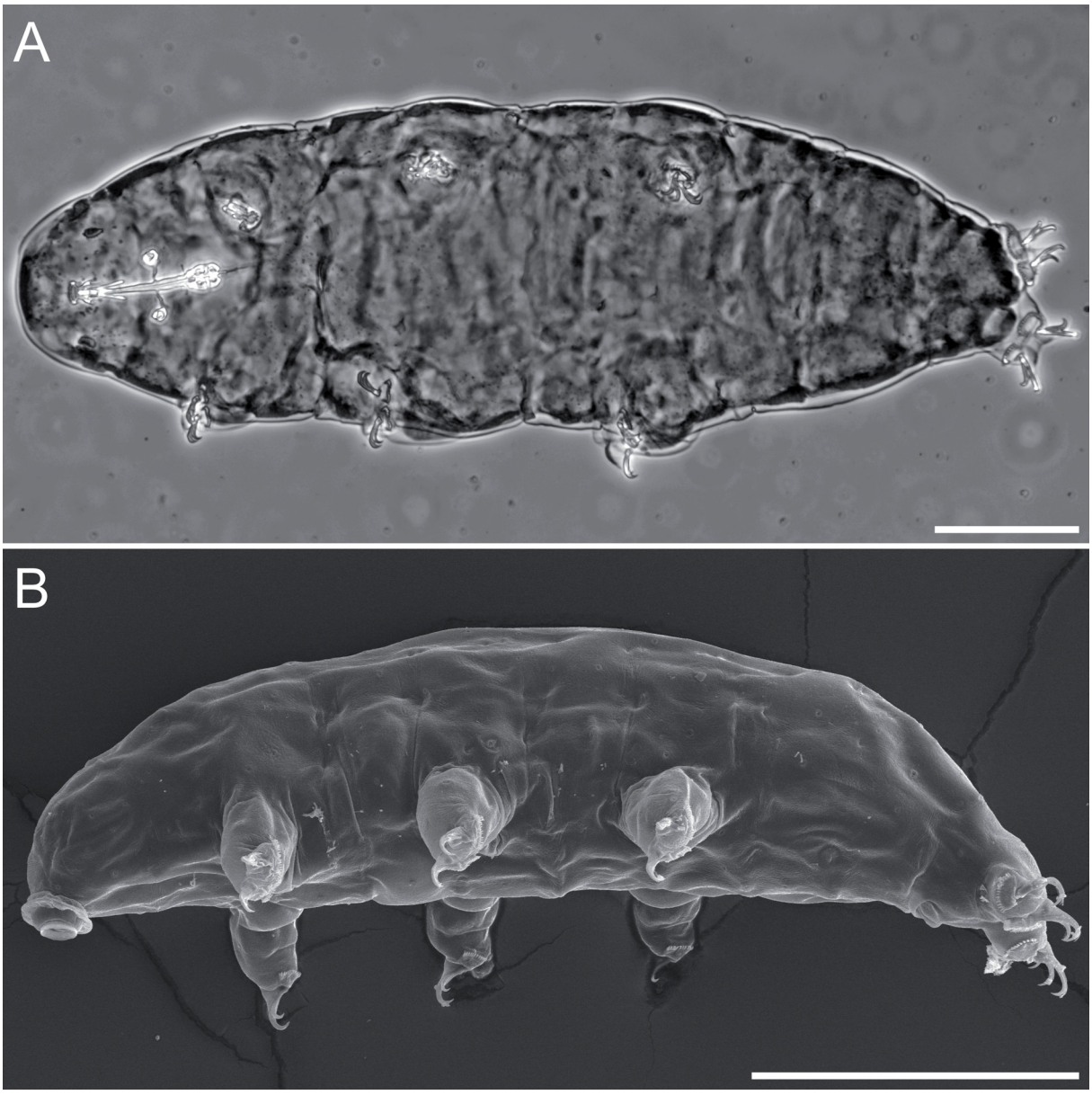

Fig. 8. *Richtersius ingemari* sp. nov. from sample SE.002 (holotype and paratype ISEA-PAS), habitus. **A**. Adult holotype habitus (PCM). **B**. Newborn paratype habitus (SEM). Scale bars = 100 µm.

Etymology

This species is named after Prof. Ingemar Jönsson of Kristianstad University, Sweden, in recognition of his efforts in studying the physiological adaptations of tardigrades to extreme conditions, utilizing this species as a model organism.

Type material

Holotype

SWEDEN • Öland Island; 56°32′18.2″ N, 16°27′45.3″ E; 46 m a.s.l.; Oct. 2006; R.M. Kristensen leg.; moss on rock; ISEA-PAS, slide SE.002.5.

Paratypes

SWEDEN • 69 specs; same data as for holotype; ISEA PAS, slides SE.002.1 to SE.002.7, SEM stubs TAR.2.01, TAR.2.02 • 44 eggs; same data as for holotype; ISEA PAS, slides SE.002.13, SE.002.14, SEM stubs TAR.2.01, TAR.2.02 • 22 specs; same data as for holotype; MUC, slides NHMD-1732287, NHMD-1732288 • 41 eggs; same data as for holotype; MUC, slides NHMD-1732289 to NHMD-1732291.

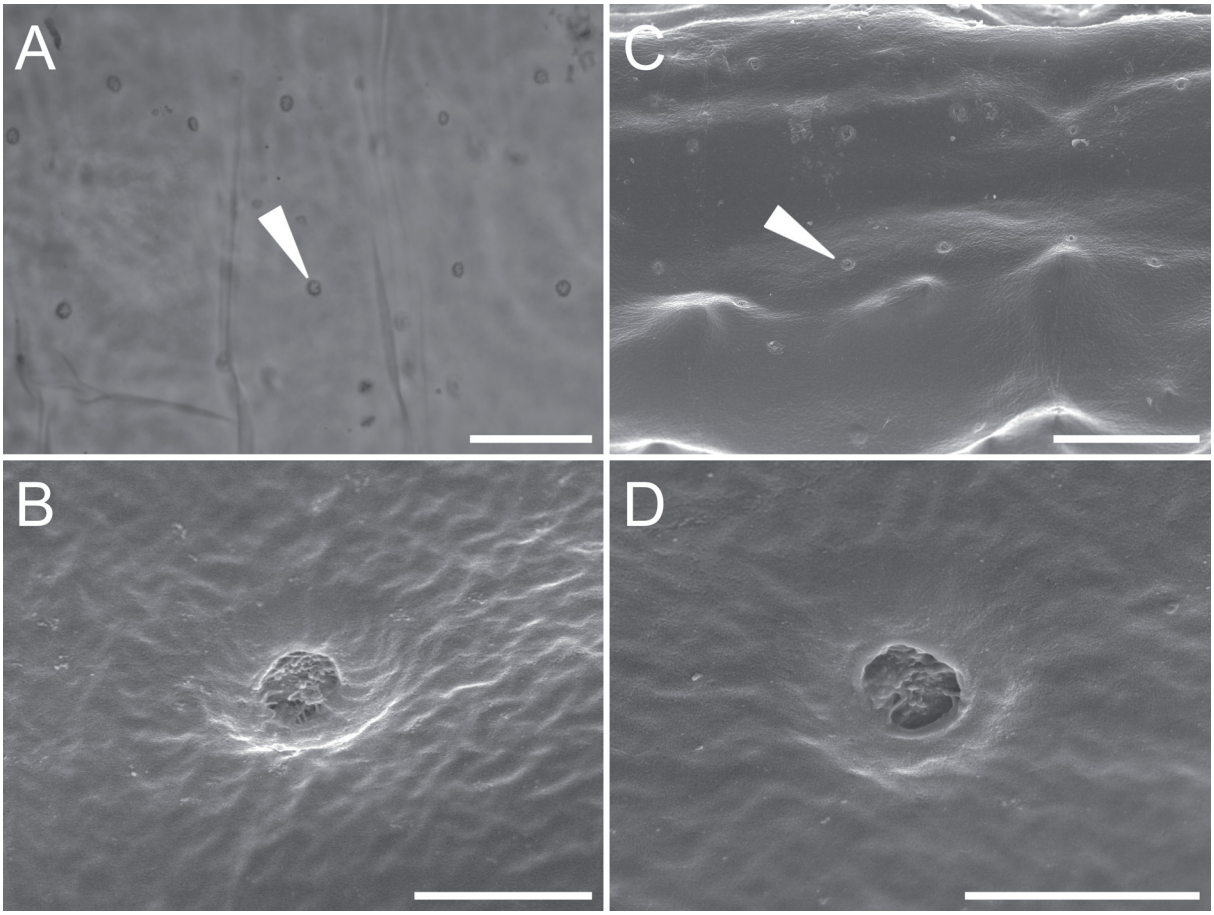

Fig. 9. Newborn *Richtersius ingemari* sp. nov. from sample SE.002 (paratypes ISEA-PAS), cuticular pores in newborns. **A**. Dorso-caudal cuticle with pores (PCM). **C**. Dorso-caudal cuticle with pores (PCM). **B, D**. Pores (SEM). Arrowheads indicate pores on the cuticle. Scale bars: A, C = 20 μm; B, D = 2 μm.

Table 6 (continued on next page). Measurements (in µm) and *pt* values of selected morphological structures of adults of *Richtersius ingemari* sp. nov. excluding hatchlings. Specimens mounted in Hoyer's medium. Range refers to the smallest and the largest structure among all measured specimens. Abbreviations; N = number of specimens/structures measured; SD = standard deviation).

Character	N	Range		Mean		SD		Holotype	
		µm	*pt*	µm	*pt*	µm	*pt*	µm	*pt*
Body length	21	441 – 742	*688 – 975*	632	*863*	71	*72*	742	*964*
Buccal tube									
Buccal tube length	24	62.0 – 79.2	–	72.3	–	5.0	–	77.0	–
Stylet support insertion point	21	44.6 – 56.8	68.1 – 73.8	51.2	71.1	3.8	1.6	54.2	*70.4*
Buccal tube external width	22	4.2 – 6.8	*6.0 – 9.4*	5.7	*7.8*	0.8	*0.9*	6.0	*7.8*
Buccal tube internal width	22	1.2 – 1.9	*1.6 – 2.7*	1.6	*2.2*	0.2	*0.3*	1.5	*2.0*
Ventral lamina length	10	22.5 – 27.3	*29.4 – 42.5*	24.6	*34.0*	1.9	*4.1*		
Placoid lengths									
Macroplacoid 1	19	6.6 – 8.9	*9.4 – 12.7*	7.9	*10.9*	0.7	*0.8*	8.3	*10.8*
Macroplacoid 2	21	6.3 – 9.0	*8.4 – 13.0*	7.5	*10.4*	0.8	*1.0*	8.4	*10.8*
Placoid row	19	14.2 – 19.3	*20.7 – 26.5*	17.3	*23.7*	1.4	*1.4*	18.6	*24.2*
Claw I heights									
External base	9	8.7 – 16.9	*11.6 – 22.0*	12.0	*16.3*	2.6	*3.3*	16.9	*22.0*
External primary branch	12	16.0 – 23.0	*24.0 – 30.2*	19.9	*27.1*	2.1	*2.3*	23.0	*29.9*
External secondary branch	12	12.1 – 19.8	*18.9 – 26.3*	16.9	*22.9*	2.3	*2.5*	19.2	*25.0*
External base/primary branch (*cct*)	9	39.4 – 73.4	–	59.6	–	12.4	–	73.4	–
Internal base	9	8.4 – 16.3	*11.1 – 21.2*	11.7	*16.0*	2.6	*3.1*	16.3	*21.2*
Internal primary branch	13	15.7 – 24.7	*22.3 – 34.0*	19.9	*27.1*	2.7	*3.3*	21.7	*28.2*
Internal secondary branch	13	11.7 – 19.8	*18.2 – 27.2*	16.4	*22.3*	2.6	*3.0*	18.6	*24.2*
Internal base/primary branch (*cct*)	9	38.0 – 75.3	–	60.2	–	10.4	–	75.3	–
Claw II heights									
External base	10	10.5 – 16.5	*14.9 – 21.4*	12.5	*17.6*	1.9	*1.8*	16.5	*21.4*
External primary branch	15	16.1 – 24.6	*24.6 – 33.7*	20.7	*28.6*	2.3	*2.8*	24.6	*32.0*
External secondary branch	15	12.6 – 20.1	*19.6 – 29.5*	17.3	*23.9*	2.4	*2.9*	20.1	*26.1*
External base/primary branch (*cct*)	10	46.7 – 68.7	–	61.3	–	6.7	–	66.8	–
Internal base	13	9.1 – 15.2	*14.7 – 20.3*	12.6	*17.5*	1.7	*1.7*	15.2	*19.7*
Internal primary branch	16	16.0 – 24.0	*24.1 – 34.5*	20.6	*28.7*	2.5	*3.3*	24.0	*31.2*
Internal secondary branch	16	12.1 – 19.5	*19.0 – 27.2*	16.6	*23.0*	2.2	*2.7*	18.5	*24.0*
Internal base/primary branch (*cct*)	13	49.6 – 69.7	–	61.7	–	6.6	–	63.3	–
Claw III heights									
External base	11	11.1 – 17.4	*14.2 – 22.5*	13.4	*18.3*	2.1	*2.4*	17.4	*22.5*
External primary branch	14	19.2 – 24.7	*26.1 – 34.1*	22.0	*30.2*	1.9	*2.4*	24.7	*32.0*
External secondary branch	14	15.0 – 21.0	*21.1 – 28.4*	18.5	*25.4*	1.6	*2.0*	19.8	*25.7*
External base/primary branch (*cct*)	11	45.7 – 75.6	–	61.0	–	8.5	–	70.3	–
Internal base	10	9.5 – 15.7	*12.6 – 20.4*	12.5	*16.8*	2.1	*2.4*	15.7	*20.4*
Internal primary branch	12	18.7 – 24.7	*25.2 – 34.6*	21.6	*29.4*	2.1	*2.7*	23.8	*30.9*
Internal secondary branch	12	13.6 – 20.5	*19.3 – 26.6*	17.3	*23.6*	2.1	*2.4*	18.5	*24.0*
Internal base/primary branch (*cct*)	10	48.2 – 66.2	–	57.6	–	7.4	–	66.0	–

Table 6 (continued). Measurements (in µm) and *pt* values of selected morphological structures of adults of *Richtersius ingemari* sp. nov. excluding hatchlings. Specimens mounted in Hoyer's medium. Range refers to the smallest and the largest structure among all measured specimens. Abbreviations; N = number of specimens/structures measured; SD = standard deviation.

Character	N	Range		Mean		SD		Holotype	
		µm	*pt*	µm	*pt*	µm	*pt*	µm	*pt*
Claw IV heights									
Anterior base	12	12.5 – 21.1	*17.6 – 27.3*	16.9	*22.4*	2.6	*3.2*	21.1	*27.3*
Anterior primary branch	17	21.8 – 32.2	*31.9 – 44.3*	27.5	*37.0*	3.1	*3.6*	32.2	*41.8*
Anterior secondary branch	17	15.6 – 23.9	*23.8 – 34.2*	20.8	*28.3*	2.4	*3.2*	21.1	*27.3*
Anterior base/primary branch (*cct*)	12	50.8 – 69.2	–	59.8	–	5.2	–	65.4	–
Posterior base	14	12.0 – 19.4	*17.3 – 26.5*	16.6	*22.4*	2.5	*3.2*	19.4	*25.2*
Posterior primary branch	17	21.8 – 33.0	*31.6 – 45.6*	27.8	*37.4*	3.2	*3.9*	33.0	*42.8*
Posterior secondary branch	17	12.9 – 25.4	*20.1 – 35.2*	21.6	*29.2*	3.3	*4.0*	24.2	*31.4*
Posterior base/primary branch (*cct*)	14	41.0 – 69.6	–	58.6	–	7.9	–	58.8	–
Number of teeth on internal lunula III	8	10 – 15		12.0		1.4			
Number of teeth on external lunula III	7	9 – 11		10.1		0.7		10	
Number of teeth on anterior lunula IV	10	9 – 11		9.8		0.8		11	
Number of teeth on posterior lunula IV	11	11 – 22		15.1		3.1		15	

Description

Animals (measurements in Tables 6–7; Supp. files 3, 4)

Body is bright yellow; all specimens became transparent after the fixation in Hoyer's medium (Fig. 8). Eyes were visible in all of the animals (excluding hatchlings) mounted in Hoyer's medium. Body and leg cuticle is without granulation in all life stages and with pores present only in hatchlings (Figs 8B, 9). Hatchlings are similar in appearance to adults, except for a smaller body size and roundish pores (1.5–3.1 µm in diameter) with usually jagged edges, visible under PCM, scattered randomly throughout the body cuticle, with a mean pore density of 5 (range 4–7) per 2500 µm^2 of the dorsal cuticle (Fig. 9).

Claws are slender, primary branches with distinct accessory points (Fig.10) and an internal system of septa as described for *Richtersius coronifer* s. lat. by Lisi *et al.* (2020). The claw common tract index has an average value between 57% and 61% across all four leg pairs, meaning that the basal portion of the claw is usually longer than half the total length of the primary branch. Lunulae are large, with a crown of long, numerous and densely arranged spikes (Fig. 10). All the lunulae are trapezoidal (Fig. 10). Double muscle attachments in legs I–III and horseshoe structures in legs IV are visible in PCM, whereas cuticular bars are absent (Fig. 10).

Mouth is antero-ventral. The buccal apparatus is of the *Richtersius* type (Fig. 11). The oral cavity is followed by a system of large apophyses that form a buccal crown (Fig. 11A–B). Anteriorly, the system consists of dorso-lateral and ventro-lateral triangular apophyses (Fig. 11A). The dorsal and ventral apophyses are composed of anteriorly positioned large cuticular hooks, followed by longitudinal crests (Fig. 11B). The hook in the ventral apophyses is smaller than the dorsal hook (Fig. 11B). The wall of the buccal tube exhibits a variable thickness (Fig. 11A), but the internal diameter of the buccal tube is almost uniformly narrow (Fig. 11A). From the mouth opening to the stylet support insertion point, the thickness of the buccal tube wall increases only slightly, while below this point the evident posterior thickness is clearly visible (Fig. 11A). The pharynx is spherical, with bilobed apophyses, three anterior cuticular spikes (typically only two are visible in any given plane, Fig. 11A) and two granular macroplacoids (2 < 1). The first and second macroplacoids have a faint constriction positioned centrally

and subterminally, respectively (Fig. 11C). The oral cavity armature is faintly visible under PCM, with only the second band of teeth visible mainly in the larger specimens (Fig. 11B). Under PCM, the second band of teeth is visible as several irregular rows of densely packed and faint dark dots (Fig. 11B). The discontinuous third band of teeth is situated between the second band of teeth and the opening of the buccal tube and is divided into a dorsal and a ventral portion, both in the form of a single large tooth resembling a beak.

Eggs (measurements in Table 8; Supp. file 3)
Large, roundish, yellow, laid freely. The surface between processes is smooth but with refracting dots faintly visible only under PCM, but difficult to observe because of the amount of debris that is typically attached to the egg surface (Figs 12–13). Processes in the shape of elongated, thin, cones with a ragged surface caused by small granules visible both in LM and SEM (Figs 12, 13B). The processes are sometimes bifurcated (Figs 12E–F, 13B). A ring of small pores visible only with SEM is present around each process (Fig. 13C). The processes are hollow inside (Fig. 13D). Terminal discs or other structures absent.

Reproduction
Thelytokous parthenogenesis, chromosome number 2n = 12 (Rebecchi *et al.* 2003; Stec *et al.* 2020b). Automictic parthenogenesis has been suggested for this species by Rebecchi *et al.* (2003) based on the presence of chiasmata in the oocytes.

DNA sequences

– 18S: AY582121, KT778706-7 (Guidetti *et al.* 2016), MH681761-2 (Stec *et al.* 2020b)
– 28S: GQ849048, KT778697-8 (Guidetti *et al.* 2016), MH681758-9 (Stec *et al.* 2020b)
– COI: EU251385, EU244606, EU251383-4, MH676054-5 (Stec *et al.* 2020b), PP986907-8 (this study)
– ITS2: MH681764-5 (Stec *et al.* 2020b)

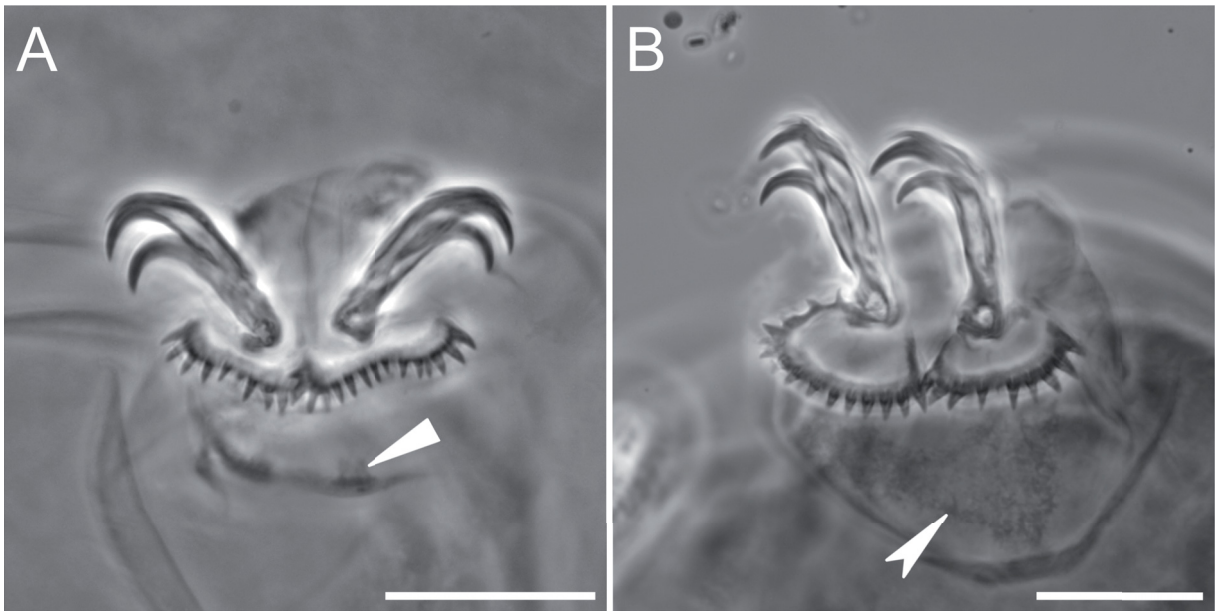

Fig. 10. Adult *Richtersius ingemari* sp. nov. from sample SE.002 (paratypes ISEA-PAS), claws and associated structures. **A**. Claws I (PCM). **B**. Claws IV (PCM).). Arrowhead indicates muscle attachments. Indented arrowhead indicates horseshoe structure under claws IV. Scale bars = 20 µm.

Table 7 (continued on next page). Measurements (in µm) and *pt* values of selected morphological structures of hatchlings of *Richtersius ingemari* sp. nov. Specimens mounted in Hoyer's medium. Range refers to the smallest and the largest structure among all measured specimens. Abbreviations: N = number of specimens/structures measured; SD = standard deviation. * when N = 1, the mean is the measurement.

Character	N	Range		Mean*		SD	
		µm	*pt*	µm	*pt*	µm	*pt*
Body length	2	457 – 502	*750 – 750*	480	*750*	32	
Buccal tube							
Buccal tube length	1			66.9			
Stylet support insertion point	1			48.0	*71.7*		
Buccal tube external width	1			4.2	*6.3*		
Buccal tube internal width	1			1.5	*2.3*		
Ventral lamina length	0						
Placoid lengths							
Macroplacoid 1	1			7.3	*10.9*		
Macroplacoid 2	1			6.7	*10.0*		
Placoid row	1			16.0	*23.8*		
Claw I heights							
External base	1			8.1	*12.1*		
External primary branch	1			15.2	*22.6*		
External secondary branch	1			12.4	*18.5*		
External base/primary branch (*cct*)	1			53.6	–		
Internal base	1			8.3	*12.3*		
Internal primary branch	1			14.7	*21.9*		
Internal secondary branch	1			11.0	*16.4*		
Internal base/primary branch (*cct*)	1			56.2	–		
Claw II heights							
External base	1			7.6	*11.3*		
External primary branch	1			15.2	*22.7*		
External secondary branch	1			11.3	*16.9*		
External base/primary branch (*cct*)	1			49.6	–		
Internal base	1			8.7	*13.0*		
Internal primary branch	1			14.2	*21.2*		
Internal secondary branch	1			10.4	*15.6*		
Internal base/primary branch (*cct*)	1			61.1	–		
Claw III heights							
External base	1			7.6	*11.3*		
External primary branch	1			14.5	*21.7*		
External secondary branch	1			10.8	*16.1*		
External base/primary branch (*cct*)	1			52.1	–		
Internal base	1			9.1	*13.6*		
Internal primary branch	1			14.9	*22.2*		
Internal secondary branch	1			11.0	*16.4*		
Internal base/primary branch (*cct*)	1			61.3	–		

Table 7 (continued). Measurements (in µm) and *pt* values of selected morphological structures of hatchlings of *Richtersius ingemari* sp. nov. Specimens mounted in Hoyer's medium. Range refers to the smallest and the largest structure among all measured specimens. Abbreviations: N = number of specimens/structures measured; SD = standard deviation. * when N = 1, the mean is the measurement.

Character	N	Range		Mean*		SD	
		µm	*pt*	µm	*pt*	µm	*pt*
Claw IV heights							
Anterior base	0						
Anterior primary branch	0						
Anterior secondary branch	0						
Anterior base/primary branch (*cct*)	0						
Posterior base	0						
Posterior primary branch	0						
Posterior secondary branch	0						
Posterior base/primary branch (*cct*)	0						
Number of teeth on internal lunula III	2	10 – 12		11.0		1.4	
Number of teeth on external lunula III	2	12 – 13		12.5		0.7	
Number of teeth on anterior lunula IV	0						
Number of teeth on posterior lunula IV	0						
Pore density (PD)	3	4 – 7		5.0		1.7	
Pore size	30	1.5 – 3.1		2.3		0.4	

Table 8. Measurements (in µm) of the eggs of *Richtersius ingemari* sp. nov. Eggs mounted in Hoyer's medium; process base/height ratio is expressed as percentage. Range refers to the smallest and the largest structure among all measured specimens. Abbreviations: N = number of eggs/structures measured; SD = standard deviation.

Character	N	Range	Mean	SD
Egg bare diameter	13	114.8 – 137.2	129.3	6.0
Egg full diameter	13	150.5 – 184.0	168.9	9.0
Process height	39	8.9 – 28.9	18.4	4.3
Process base width	39	2.3 – 6.4	4.3	0.9
Process base/height ratio	39	16% – 32%	24%	4%
Inter-process distance	39	5.1 – 13.7	8.6	1.8
Number of processes on the egg circumference	13	27 – 33	30.2	1.5

Distribution

Locus typicus: Möckelmossen, Öland Island, Sweden (56°32′18.2″ N, 16°27′45.3″ E). Moss on tock (sample SE.002 in this study).

Möckelmossen, Öland Island, Sweden (56°31.732′ N, 16°29.474′ E). Moss on rock(sample C2353 in Guidetti *et al.* 2016; sample P4 in Rebecchi *et al.* 2003; sample C3585-S6 in Vecchi *et al.* 2018). This population has been extensively used in studies on cytology, physiology, and ecology under the name of *Richtersius coronifer*.

Lago di Teleccio, Torino, Italy (45°28′55″ N, 7°22′22″ E; 1830 m a.s.l.). Moss (sample IT.120 in Stec *et al.* 2020b).

Sasso del Corvo, Modena, Italy (44°12.774′ N, 10°31.974′ E, 1280 m a.s.l.). Moss on rock (sample C3226 in Guidetti *et al*. 2016; sample P3 in Rebecchi *et al.* 2003).

Kościeliska Valley, Tatrzański National Park, Poland (49°14′22″ N, 19°51′46″ E; 1083 m a.s.l.). Moss (sample PL.246 in Stec *et al.* 2020b).

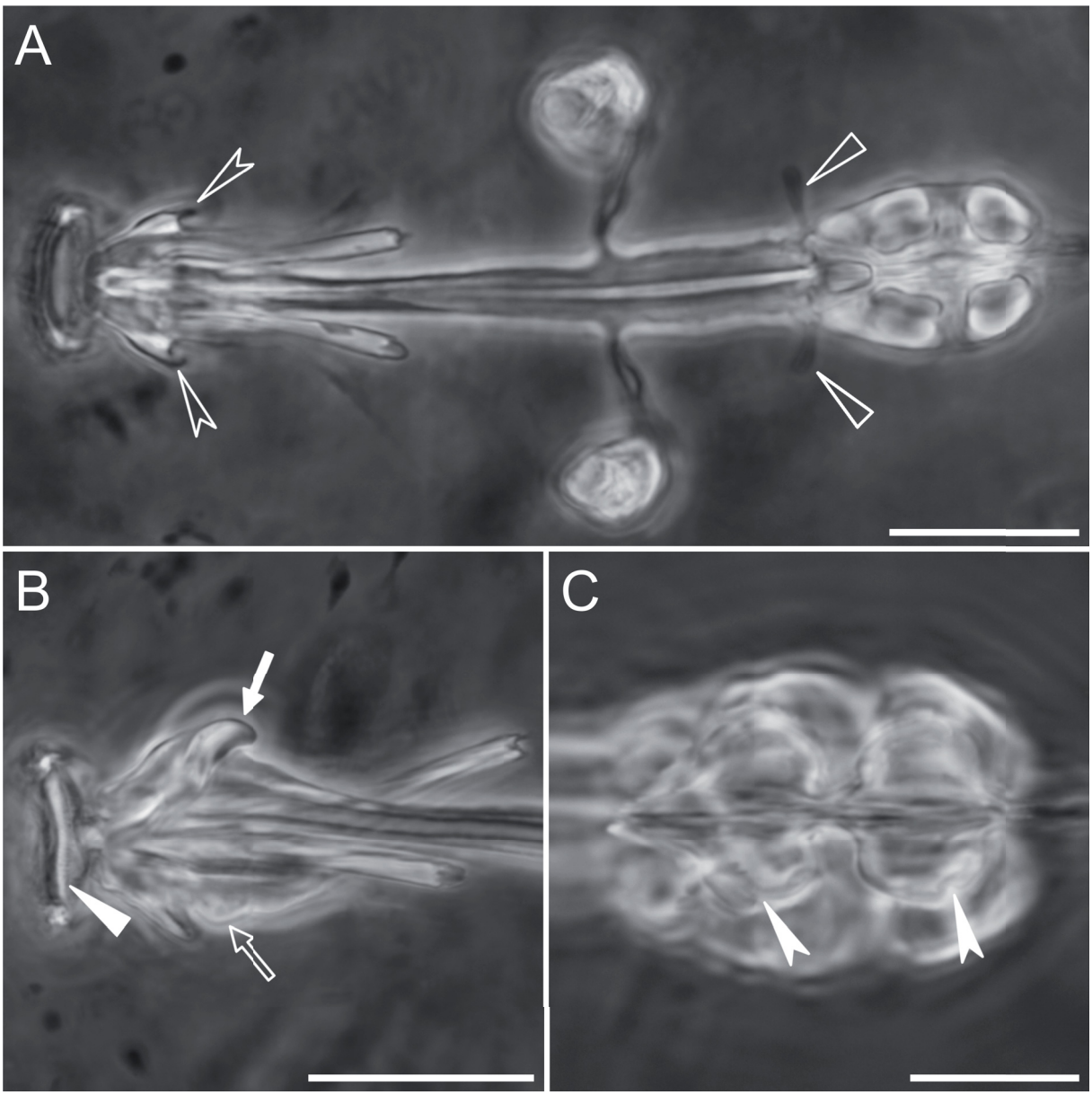

Fig. 11. Adult *Richtersius ingemari* sp. nov. from sample SE.002 (paratypes ISEA-PAS), buccal apparatus. **A**. Entire buccal apparatus (PCM). **B**. Lateral view of the buccal crown (PCM). **C**. Macroplacoids (PCM). Filled arrow indicates dorsal hook of the AISM. Empty arrow indicates ventral hook of AISM. Empty indented arrowheads indicate triangular apophyses of the buccal crown. Empty arrowheads indicate anterior cuticular spike. Filled arrowhead indicates the third OCA ring. Filled indented arrowheads indicate placoids constrictions. Scale bars: A–B = 20 μm; C = 10 μm.

Differential diagnosis

Richtersius ingemari sp. nov. differs from:

Richtersius coronifer by having smaller eggs (bare diameter 114–137 μm in *R. ingemari* sp. nov. vs 173–233 μm in *R. coronifer*) and by having a lower pore density in the newborns (PD 4–7 in *R. ingemari* vs 60–88 in *R. coronifer*).

Richtersius ziemowiti by having a lower pore density in the newborns (PD 4–7 in *R. ingemari* sp. nov. vs 20–24 in *R. ziemowiti*).

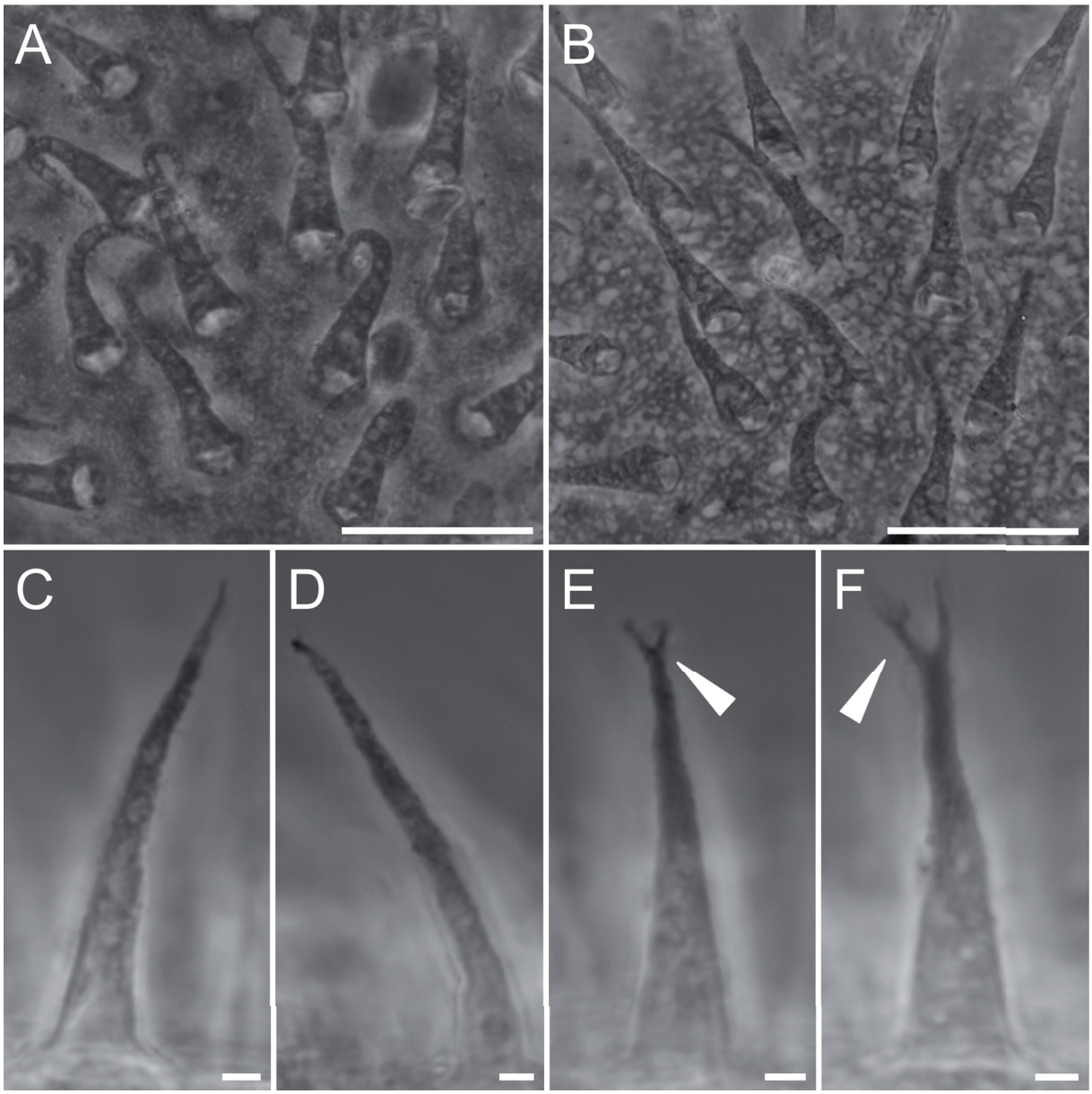

Fig. 12. Eggs of *Richtersius ingemari* sp. nov. from sample SE.002 (paratypes ISEA-PAS). **A–B**. Chorion surface and processes (PCM). **C–F**. Egg processes (PCM). Arrowheads indicate bifurcated processes. Scale bars: A–B = 20 μm: C–F = 2 μm.

Richtersius mazepi by having bigger eggs (bare diameter 114–137 µm in *R. ingemari* sp. nov. vs 77–91 µm in *R. mazepi*), by the absence of a crown of thickenings distributed around the bases of the egg processes (present in *R. mazepi*), by the different shape of the egg processes (conical spikes in *R. ingemari* vs wide dome-shaped proximal portion and an elongated slender distal portion in *R. mazepi*), by having a lower pore density in the newborns (PD 4–7 in *R. ingemari* vs 26–36 in *R. mazepi*), and by having a higher claw IV anterior *cct* (*51–69*% in *R ingemari* vs *32–44*% in *R. mazepi*).

Richtersius tertius by having a smaller first macroplacoid (*pt 9–13* in *R. ingemari* sp. nov. vs *14–20* in *R. tertius*).

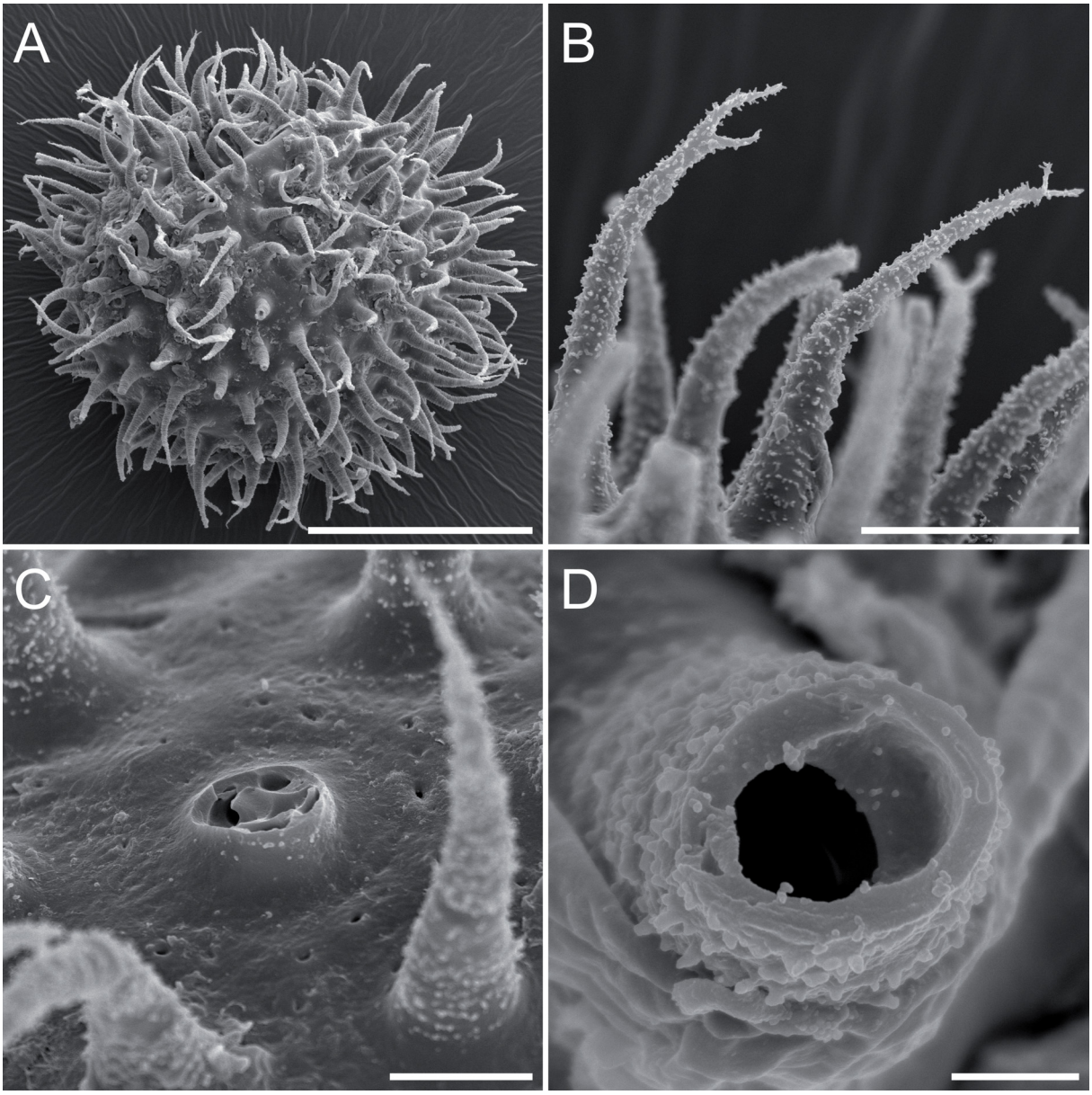

Fig. 13. Eggs of *Richtersius ingemari* sp. nov. from sample SE.002 (paratypes ISEA-PAS). **A**. Egg in toto (SEM). **B**. Egg processes (SEM). **C–D**. Egg processes sections (SEM). Scale bars: A = 50 µm; B = 10 µm; C = 5 µm; D = 1 µm.

Richtersius nicolai sp. nov. by having a higher pore density in the newborns (PD 4–7 in *R. ingemari* sp. nov. vs 9–11 in *R. nicolai*), and by the reproductive mode (parthenogenesis in *R. ingemari* vs gonochorism in *R. nicolai*).

Richtersius sp. [Ca1 MK214326]

Richtersius sp. 6 – Stec *et al.* 2020b.

Description

No information on this species morphology is available.

Reproductive mode

Gonochoric (Stec *et al.* 2020b).

DNA sequences

– 18S: MK211387 (Stec *et al.* 2020b)
– 28S: MK211385 (Stec *et al.* 2020b)
– COI: MK214326-8 (Stec *et al.* 2020b)
– ITS2: MK211382-3 (*Stec et al.* 2020b)

Distribution

Genna Silana, Sardegna, Italy (40°09′04″ N, 9°30′23″ E; 1047 m a.s.l.). Moss (sample IT.317 in Stec *et al.* 2020b).

Richtersius sp. [Ca2 KT778685]

Richtersius Mongolia – Guidetti *et al.* 2016.
Richtersius sp. 2 – Stec *et al.* 2020b.

Description

In the newborns, many small cuticular pores (diameter 1–2 µm) with regular margins are present. Claw common tract shorter than half of the total claw length. The buccal tube walls are extremely enlarged after the stylet support insertions (Guidetti *et al.* 2016). Additional morphometric data for this species are presented in Guidetti *et al.* (2016).

Reproductive mode

Gonochoric (Guidetti *et al.* 2016).

DNA sequences

– 18S: KT778708-10 (Guidetti *et al.* 2016)
– 28S: KT778699-701 (Guidetti *et al.* 2016)
– COI: KT778683-9 (Guidetti *et al.* 2016)

Distribution

Mongolia (46°47.311′ N, 101°57.848′ E; 1790 m a.s.l.). Moss (samples C2592 and C2595 in Guidetti *et al.* 2016).

Richtersius sp. [Ca3 GU237485]

Description

No information on this species morphology is available.

Reproductive mode

Unknown.

DNA sequences

– COI: GU237485, GU339056 (unpublished).

Distribution

Unpublished, probably Asia.

Dichotomous key of the genus Richtersius

Here we provide a taxonomic key which include six nominal species that are currently recognized within the genus.

1. Egg with processes having proximal portion in shape of wide domes while distal portion elongated and slender; crown of thickenings distributed around the bases of the egg processes ..... ***Richtersius mazepi*** Kiosya & Stec, 2022
– Egg different 2

2. Egg bare diameter ≥ 170 µm; in newborns, pore density ≥ 60 pores / 2500 µm² ..... ***Richtersius coronifer*** (Richters, 1903)
– Egg bare diameter < 170 µm; in newborns, pore density < 60 pores / 2500 µm² 3

3. In newborns, pore density ≥ 20 pore / 2500 µm² ..... ***Richtersius ziemowiti*** Kayastha *et al.*, 2020
– In newborns, pore density < 20 pore / 2500 µm² 4

4. In newborns, pore density ≥ 9 pore / 2500 µm² ..... ***Richtersius nicolai*** sp. nov.
– In newborns, pore density ≤ 7 pore / 2500 µm² 5

5. Macroplacoid 1 *pt > 13* ..... ***Richtersius tertius*** Pogwizd & Stec, 2022
– Macroplacoid 1 *pt < 13* ..... ***Richtersius ingemari*** sp. nov.

Discussion

We showed that our study, framed within the integrative taxonomy approach, allows us to confidently identify new species of the genus *Richtersius*. The new species of *Richtersius* described here has had its genetic identity known for almost two decades, but formal naming and characterization were possible only now after careful comparative analysis of its phenotypes and phylogenetic position. For decades *Richtersius* consisted of only one nominal species, and after its redescription in 2020 we now have as many as six formally named taxa. Therefore, our results further exemplify that removing taxonomic obstacles by integrative redescriptions of insufficiently described taxa, especially type species, opens the window for further studies on the species diversity within a given group.

We would like to emphasize that caution is required for future species identification of populations within the genus *Richtersius*. As evident in the dichotomous key provided above, the identification of these taxa typically requires examination of eggs, newborns, and adult animals. Therefore, we recommend comparing all these life stages to avoid false inferences about crypsis. Cryptic speciation, which may occur within this genus, can complicate comparative biology studies (Caputi *et al.* 2007), as experimental results from different cryptic species can vary. Given that the genus *Richtersius* has been extensively utilized in studies on the physiology of cryptobiosis, results obtained from different populations should be compared with care (Bortolus 2008). When species description is not feasible

due to resource limitation, the use of parallel informal nomenclatural schemes such as the unconfirmed candidate species (UCS) approach proposed by Padial *et al.* (2010) is a promising alternative: it provides standardized container names where to gather the information on several traits (e.g., ecology, morphology physiology) of not yet formally described species-level entities.

Acknowledgments

Sample IT.137 was collected in a national park under Sampling permit AOO_05_054/017/2023 from Parco Nazionale del Gargano (FG), Italy. This study received support from the European Commission's program 'Transnational Access to Major Research Infrastructures' through the SYNTHESYS grant no. DK-TAF-TA4-005 to DS and from the Academy of Finland Fellowship to SC (#314219 and #335759). We wish to thank Prof. Izabela Poprawa and Dr Izabela Potocka (University of Silesia, Katowice, Poland) for assistance in acquiring SEM photographs. We also wish to thank Diane Nelson and an anonymous reviewer for their constructive comments.

References

Bertolani R., Guidetti R., Marchioro T., Altiero T., Rebecchi L. & Cesari M. 2014. Phylogeny of Eutardigrada: New molecular data and their morphological support lead to the identification of new evolutionary lineages. *Molecular Phylogenetics and Evolution* 76 (1): 110–126. https://doi.org/10.1016/j.ympev.2014.03.006

Bortolus A. 2008. Error cascades in the biological sciences: The unwanted consequences of using bad taxonomy in ecology. *AMBIO: A Journal of the Human Environment* 37 (2): 114–118. https://doi.org/10.1579/0044-7447(2008)37[114:ECITBS]2.0.CO;2

Camarda D., Massa E., Guidetti R. & Lisi O. 2023. A new, simplified, drying protocol to prepare tardigrades for scanning electron microscopy. *Microscopy Research and Technique* 87 (4): 716–726. https://doi.org/10.1002/jemt.24460

Caputi L., Andreakis N., Mastrototaro F., Cirino P., Vassillo M. & Sordino P. 2007. Cryptic speciation in a model invertebrate chordate. *Proceedings of the National Academy of Sciences* 104 (22): 9364–9369. https://doi.org/10.1073/pnas.0610158104

Casquet J.T., Thebaud C. & Gillespie R.G. 2012. Chelex without boiling, a rapid and easy technique to obtain stable amplifiable DNA from small amounts of ethanol-stored spiders. *Molecular Ecology Resources* 12 (1): 136–141. https://doi.org/10.1111/j.1755-0998.2011.03073.x

Czernekova M. & Jönsson K.I. 2016. Experimentally induced repeated anhydrobiosis in the eutardigrade *Richtersius coronifer*. *PLoS ONE* 11 (11): e0164062. https://doi.org/10.1371/journal.pone.0164062

Czerneková M., Jönsson K.I., Chajec L., Student S. & Poprawa I. 2017. The structure of the desiccated *Richtersius coronifer* (Richters, 1903). *Protoplasma* 254 (3): 1367–1377. https://doi.org/10.1007/s00709-016-1027-2

Czerneková M., Janelt K., Student S., Jönsson K.I. & Poprawa I. 2018. A comparative ultrastructure study of storage cells in the eutardigrade *Richtersius coronifer* in the hydrated state and after desiccation and heating stress. *PLoS ONE* 13 (8): e0201430. https://doi.org/10.1371/journal.pone.0201430

Dunn C.W., Hejnol A., Matus D.Q., Pang K., Browne W.E., Smith S.A., Seaver E., Rouse G.W., Obst M., Edgecombe G.D., Sørensen M.V., Haddock S.H.D., Schmidt-Rhaesa A., Okusu A., Kristensen R.M., Wheeler W.C., Martindale M.Q. & Giribet G. 2008. Broad phylogenomic sampling improves resolution of the animal tree of life. *Nature* 452 (7188): 745–749. https://doi.org/10.1038/nature06614

Edgar R.C. 2004. MUSCLE: Multiple sequence alignment with high accuracy and high throughput. *Nucleic Acids Research* 32 (5): 1792–1797. https://doi.org/10.1093/nar/gkh340

Faurby S., Jönsson K.I., Rebecchi L. & Funch P. 2008. Variation in anhydrobiotic survival of two eutardigrade morphospecies: A story of cryptic species and their dispersal. *Journal of Zoology* 275 (2): 139–145. https://doi.org/10.1111/j.1469-7998.2008.00420.x

Guidetti R., Gandolfi A., Rossi V. & Bertolani R. 2005. Phylogenetic analysis of Macrobiotidae (Eutardigrada, Parachela): A combined morphological and molecular approach. *Zoologica Scripta* 34 (3): 235–244. https://doi.org/10.1111/j.1463-6409.2005.00193.x

Guidetti R., Rebecchi L., Bertolani R., Jönsson K.I., Kristensen R.M. & Cesari M. 2016. Morphological and molecular analyses on *Richtersius* (Eutardigrada) diversity reveal its new systematic position and lead to the establishment of a new genus and a new family within Macrobiotoidea. *Zoological Journal of the Linnean Society* 178 (4): 834–845. https://doi.org/10.1111/zoj.12428

Guidetti R., Vecchi M., Ferrari A., Newton I.L., Cesari M. & Rebecchi L. 2019. Further insights in the Tardigrada microbiome: Phylogenetic position and prevalence of infection of four new Alphaproteobacteria putative endosymbionts. *Zoological Journal of the Linnean Society* 188 (3): 925–937. https://doi.org/10.1093/zoolinnean/zlz128

Guidetti R., Schill R.O., Giovannini I., Massa E., Goldoni S.E., Ebel C., Förschler M.I., Rebecchi L. & Cesari M. 2021. When DNA sequence data and morphological results fit together: Phylogenetic position of *Crenubiotus* within Macrobiotoidea (Eutardigrada) with description of *Crenubiotus ruhesteini* sp. nov. *Journal of Zoological Systematics and Evolutionary Research* 59 (3): 576–587. https://doi.org/10.1111/jzs.12449

Hagelbäck P. & Jönsson K.I. 2023. An experimental study on tolerance to hypoxia in tardigrades. *Frontiers in Physiology* 14: 1249773. https://doi.org/10.3389/fphys.2023.1249773

Halberg K.A., Larsen K.W., Jørgensen A., Ramløv H. & Møbjerg N. 2012. Inorganic ion composition in Tardigrada: Cryptobionts contain large fraction of unidentified organic solutes. *Journal of Experimental Biology* 216 (7): 1235–1243. https://doi.org/10.1242/jeb.075531

Halberg K.A., Jørgensen A. & Møbjerg N. 2013. Desiccation tolerance in the tardigrade *Richtersius coronifer* relies on muscle mediated structural reorganization. *PLoS ONE* 8 (12): e85091. https://doi.org/10.1371/journal.pone.0085091

Hindborg Mortensen L., Lynge Nilsson L., Nyby C. & Vilstrup A. 2010. *Quantifying 8-hydroxy-2'-deoxyguanosine with Enzyme-linked Immunosorbent Assay (ELISA) as a Measure of DNA Damage in the Eutardigrade Richtersius coronifer*. Report, Roskilde University, Roskilde. Available from https://rucforsk.ruc.dk/ws/portalfiles/portal/57743684/samlet.pdf [accessed 14 Feb. 2025].

Ivarsson H. & Jönsson K.I. 2004. Aggregation effects on anhydrobiotic survival in the tardigrade *Richtersius coronifer*. *Journal of Experimental Zoology Part A: Comparative Experimental Biology* 301A (2): 195–199. https://doi.org/10.1002/jez.a.20018

Jönsson K.I. 2007. Long-term experimental manipulation of moisture conditions and its impact on moss-living tardigrades. *Journal of Limnology* 66 (s1): 119–125. https://doi.org/10.4081/jlimnol.2007.s1.119

Jönsson K.I. & Guidetti R. 2001. Effects of methyl bromide fumigation on anhydrobiotic micrometazoans. *Ecotoxicology and Environmental Safety* 50 (1): 72–75. https://doi.org/10.1006/eesa.2001.2090

Jönsson K.I. & Rebecchi L. 2002. Experimentally induced anhydrobiosis in the tardigrade *Richtersius coronifer*: Phenotypic factors affecting survival. *Journal of Experimental Zoology* 293 (6): 578–584. https://doi.org/10.1002/jez.10186

Jönsson K.I. & Schill R.O. 2007. Induction of Hsp70 by desiccation, ionising radiation and heat-shock in the eutardigrade *Richtersius coronifer*. *Comparative Biochemistry and Physiology Part B: Biochemistry and Molecular Biology* 146 (4): 456–460. https://doi.org/10.1016/j.cbpb.2006.10.111

Jönsson K.I., Borsari S. & Rebecchi L. 2001. Anhydrobiotic survival in populations of the tardigrades *Richtersius coronifer* and *Ramazzottius oberhaeuseri* from Italy and Sweden. *Zoologischer Anzeiger* 240 (3–4): 419–423. https://doi.org/10.1078/0044-5231-00050

Jönsson K.I., Harms-Ringdahl M. & Torudd J. 2005. Radiation tolerance in the eutardigrade *Richtersius coronifer*. *International Journal of Radiation Biology* 81 (9): 649–656. https://doi.org/10.1080/09553000500368453

Jørgensen A. & Kristensen R.M. 2004. Molecular phylogeny of Tardigrada—investigation of the monophyly of Heterotardigrada. *Molecular Phylogenetics and Evolution* 32 (2): 666–670. https://doi.org/10.1016/j.ympev.2004.04.017

Kamilari M., Jørgensen A., Schiøtt M. & Møbjerg N. 2019. Comparative transcriptomics suggest unique molecular adaptations within tardigrade lineages. *BMC Genomics* 20 (1): 607. https://doi.org/10.1186/s12864-019-5912-x

Katoh K. & Toh H. 2008. Recent developments in the MAFFT multiple sequence alignment program. *Briefings in Bioinformatics* 9 (4): 286–298. https://doi.org/10.1093/bib/bbn013

Katoh K., Misawa K., Kuma K.I. & Miyata T. 2002. MAFFT: A novel method for rapid multiple sequence alignment based on fast Fourier transform. *Nucleic Acids Research* 30 (14): 3059–3066. https://doi.org/10.1093/nar/gkf436

Kayastha P., Berdi D., Mioduchowska M., Gawlak M., Łukasiewicz A., Gołdyn B., Jędrzejewski S. & Kaczmarek Ł. 2020. Description and molecular characterization of *Richtersius ziemowiti* sp. nov. (Richtersiidae) from Nepal (Asia) with evidence of heterozygous point mutation events in the 28S rRNA. *Annales Zoologici* 70 (3): 381–396. https://doi.org/10.3161/00034541ANZ2020.70.3.010

Kiosya Y. & Stec D. 2022. New species of the genus *Richtersius* Pilato & Binda, 1989 (Tardigrada: Eutardigrada: Richtersiusidae) from Uzbekistan. *Folia Biologica* 70 (4): 141–150. https://doi.org/10.3409/fb_70-4.18

Kiosya Y., Pogwizd J., Matsko Y., Vecchi M. & Stec D. 2021. Phylogenetic position of two *Macrobiotus* species with a revisional note on *Macrobiotus sottilei* Pilato, Kiosya, Lisi & Sabella, 2012 (Tardigrada: Eutardigrada: Macrobiotidae). *Zootaxa* 4933 (1): 113–135. https://doi.org/10.11646/zootaxa.4933.1.5

Lanfear R., Frandsen P.B., Wright A.M., Senfeld T. & Calcott B. 2017. PartitionFinder 2: New methods for selecting partitioned models of evolution for molecular and morphological phylogenetic analyses. *Molecular Biology and Evolution* 34 (3): 772–773. https://doi.org/10.1093/molbev/msw260

Lisi O., Londoño R. & Quiroga S. 2020. Description of a new genus and species (Eutardigrada: Richtersiidae) from Colombia, with comments on the family Richtersiidae. *Zootaxa* 4822 (4): 531–550. https://doi.org/10.11646/zootaxa.4822.4.4

Massa E., Vecchi M., Calhim S. & Choong H. 2024. First records of limnoterrestrial tardigrades (Tardigrada) from Haida Gwaii, British Columbia, Canada. *The European Zoological Journal* 91 (1): 1–20. https://doi.org/10.1080/24750263.2023.2288824

Michalczyk Ł. & Kaczmarek Ł. 2013. The Tardigrada Register: A comprehensive online data repository for tardigrade taxonomy. *Journal of Limnology* 72: 175–181. https://doi.org/10.4081/jlimnol.2013.s1.e22

Mutterer J. & Zinck E. 2013. Quick-and-clean article figures with FigureJ. *Journal of Microscopy* 252 (1): 89–91. https://doi.org/10.1111/jmi.12069

Nilsson E.J.C., Ingemar Jönsson K. & Pallon J. 2010. Tolerance to proton irradiation in the eutardigrade *Richtersius coronifer* a nuclear microprobe study. *International Journal of Radiation Biology* 86 (5): 420–427. https://doi.org/10.3109/09553000903568001

Padial J M., Miralles A., De la Riva I. & Vences M. 2010. The integrative future of taxonomy. *Frontiers in Zoology* 7(1): 16. https://doi.org/10.1186/1742-9994-7-16

Pedersen B.H., Malte H., Ramløv H. & Finster K. 2020. A method for studying the metabolic activity of individual tardigrades by measuring oxygen uptake using micro-respirometry. *Journal of Experimental Biology* 223 (22): jeb233072. https://doi.org/10.1242/jeb.233072

Pedersen B.H., Malte H., Finster K. & Ramløv H. 2021. Respiration measurements of individual tardigrades of the species *Richtersius* cf. *coronifer* as a function of temperature and salinity and termination of anhydrobiosis. *Astrobiology* 21 (7): 853–865. https://doi.org/10.1089/ast.2020.2371

Persson D.K., Halberg K.A., Jørgensen A., Ricci C., Møbjerg N. & Kristensen R.M. 2011. Extreme stress tolerance in tardigrades: Surviving space conditions in low earth orbit. *Journal of Zoological Systematics and Evolutionary Research* 49 (s1): 90–97. https://doi.org/10.1111/j.1439-0469.2010.00605.x

Pilato G. 1981. Analisi di nuovi caratteri nello studio degli Eutardigradi. *Animalia* 8: 51–57.

Pilato G. & Binda M.G. 1987. *Richtersia*, nuovo genere di Macrobiotidae, e nuova definizione di *Adorybiotus* Maucci e Ramazzotti. 1981 (Eutardigrada). *Animalia* 14 (1): 147–152.

Pilato G. & Binda M.G. 1989. *Richtersius*, nuovo nome genetico in sostituzione di *Richtersia* Pilato e Binda, 1987 (Eutardigrada). *Animalia* 16: 147–148.

Pilato G. & Binda M.G. 2010. Definition of families, subfamilies, genera and subgenera of the Eutardigrada, and keys to their identification. *Zootaxa* 2404 (1): 1–54. https://doi.org/10.11646/zootaxa.2404.1.1

Pogwizd J. & Stec D. 2022. An integrative description of a new *Richtersius* species from Greece (Tardigrada: Eutardigrada: Richtersiusidae). *Acta Zoologica Academiae Scientiarum Hungaricae* 68 (1): 1–21. https://doi.org/10.17109/AZH.68.1.1.2022

Puillandre N., Brouillet S. & Achaz G. 2021. ASAP: Assemble Species by Automatic Partitioning. *Molecular Ecology Resources* 21 (2): 609–620. https://doi.org/10.1111/1755-0998.13281

Ramløv H. & Westh P. 1992. Survival of the cryptobiotic Eutardigrade *Adorybiotus coronifer* during cooling to -196°C: Effect of cooling rate, trehalose level, and short term acclimation. *Cryobiology* 29 (1): 125–130. https://doi.org/10.1016/0011-2240(92)90012-Q

Ramløv H. & Westh P. 2001. Cryptobiosis in the eutardigrade *Adorybiotus (Richtersius) coronifer*: Tolerance to alcohols, temperature and de novo protein synthesis. *Zoologischer Anzeiger* 240 (3–4): 517–523. https://doi.org/10.1078/0044-5231-00062

Rebecchi L., Rossi V., Altiero T., Bertolani R. & Menozzi P. 2003. Reproductive modes and genetic polymorphism in the tardigrade *Richtersius coronifer* (Eutardigrada, Macrobiotidae). *Invertebrate Biology* 122 (1): 19–27. https://doi.org/10.1111/j.1744-7410.2003.tb00069.x

Richters F. 1903. Nordische Tardigraden. *Zoologischer Anzeiger* 27: 168–172.

Ronquist F., Teslenko M., Van Der Mark P., Ayres D.L., Darling A., Höhna, S., Larget B., Liu L., Suchard M.A. & Huelsenbeck J.P. 2012. MrBayes 3.2: Efficient Bayesian phylogenetic inference and model choice across a large model space. *Systematic Biology* 61 (3): 539–542. https://doi.org/10.1093/sysbio/sys029

Stec D. & Michalczyk Ł. 2020. *Macrobiotus coronifer* Richters, 1903 (type species for *Richtersius* Pilato & Binda, 1989): Designating a new neotype from the original type locality described within the integrative taxonomy framework. *Zootaxa* 4858 (2): 292–294. https://doi.org/10.11646/zootaxa.4858.2.10

Stec D. & Morek W. 2022. Reaching the monophyly: Re-evaluation of the enigmatic species *Tenuibiotus hyperonyx* (Maucci, 1983) and the genus *Tenuibiotu*s (Eutardigrada). *Animals* 12 (3): 404. https://doi.org/10.3390/ani12030404

Stec D., Kristensen R.M. & Michalczyk Ł. 2020a. An integrative description of *Minibiotus ioculator* sp. nov. from the Republic of South Africa with notes on *Minibiotus pentannulatus* Londoño et al., 2017 (Tardigrada: Macrobiotidae). *Zoologischer Anzeiger* 286: 117–134. https://doi.org/10.1016/j.jcz.2020.03.007

Stec D., Krzywański Ł., Arakawa K. & Michalczyk Ł. 2020b. A new redescription of *Richtersius coronifer*, supported by transcriptome, provides resources for describing concealed species diversity within the monotypic genus *Richtersius* (Eutardigrada). *Zoological Letters* 6 (1): 2. https://doi.org/10.1186/s40851-020-0154-y

Stec D., Vecchi M., Maciejowski W. & Michalczyk Ł. 2020c. Resolving the systematics of Richtersiidae by multilocus phylogeny and an integrative redescription of the nominal species for the genus *Crenubiotus* (Tardigrada). *Scientific Reports* 10 (1): 19418. https://doi.org/10.1038/s41598-020-75962-1

Stec D., Vecchi M., Calhim S. & Michalczyk Ł. 2021. New multilocus phylogeny reorganises the family Macrobiotidae (Eutardigrada) and unveils complex morphological evolution of the *Macrobiotus hufelandi* group. *Molecular Phylogenetics and Evolution* 160: 106987. https://doi.org/10.1016/j.ympev.2020.106987

Vecchi M. & Bruneaux M. 2021. concatipede: An R package to concatenate fasta sequences easily. http://doi.org/10.5281/zenodo.5130604

Vecchi M., Newton I.G., Cesari M., Rebecchi L. & Guidetti R. 2018. The microbial community of tardigrades: Environmental influence and species specificity of microbiome structure and composition. *Microbial Ecology* 76 (2): 467–481. https://doi.org/10.1007/s00248-017-1134-4

Westh P. & Kristensen R.M. 1992. Ice formation in the freeze-tolerant eutardigrades *Adorybiotus coronifer* and *Amphibolus nebulosus* studied by differential scanning calorimetry. *Polar Biology* 12 (8): 693–699. https://doi.org/10.1007/BF00238869

Westh P. & Ramløv H. 1991. Trehalose accumulation in the tardigrade *Adorybiotus coronifer* during anhydrobiosis. *Journal of Experimental Zoology* 258 (3): 303–311. https://doi.org/10.1002/jez.1402580305

Zawierucha K., Vecchi M., Takeuchi N., Ono M. & Calhim S. 2023. Negative impact of freeze–thaw cycles on the survival of tardigrades. *Ecological Indicators* 154: 110460. https://doi.org/10.1016/j.ecolind.2023.110460

Manuscript received: 8 July 2024
Manuscript accepted: 28 October 2024
Published on: 14 March 2025
Topic editor: Magalie Castelin
Section editor: Fabio Stoch
Desk editor: Pepe Fernández

Supplementary files

Supp. file 1. Morphometric data for animals and eggs of *Richtersius nicolai* sp. nov.
https://doi.org/10.5852/ejt.2025.981.2823.12867

Supp. file 2. Morphometric data for newborns of *Richtersius nicolai* sp. nov.
https://doi.org/10.5852/ejt.2025.981.2823.12869

Supp. file 3. Morphometric data for animals and eggs of *Richtersius ingemari* sp. nov.
https://doi.org/10.5852/ejt.2025.981.2823.12871

Supp. file 4. Morphometric data for newborns of *Richtersius ingemari* sp. nov.
https://doi.org/10.5852/ejt.2025.981.2823.12873

Supp. file 5. Input file for MrBayes phylogenetic analysis.
https://doi.org/10.5852/ejt.2025.981.2823.12875

Supp. file 6. Output from ASAP species delimitation analysis.
https://doi.org/10.5852/ejt.2025.981.2823.12877